# THE TOPOLOGICAL DESIGN OF MULTIFUNCTIONAL CELLULAR METALS

**By**

**A.G. Evans*, J.W. Hutchinson****
**N.A.Fleck***, M.F.Ashby*****
**H.N.G. Wadley******

* Princeton Materials Institute, Princeton University, Princeton, NJ 08540
** Division of Engineering and Applied Sciences, Harvard University, Cambridge, MA 02138
*** Cambridge University Engineering Department, Trumpington St., Cambridge, UK.
**** Department of Materials Science and Engineering, University of Virginia, Charlottesville, VA 22903

**ABSTRACT**

The multifunctional performance of materials based on stochastic cellular metals is now documented. This article compares such materials with the projected capabilities of materials with periodic cells, configured as cores of panels, tubes and shells. The implementation opportunities are as ultra-light structure, for compact cooling, in energy absorption and vibration control. The topologies of the periodic materials comprise either lattices based on micro-trusses or linear materials with corrugated cores. Performance benefits that can be expected upon implementing these periodic materials are presented and compared with competing concepts. Methods for manufacturing these materials are discussed and some cost/performance trade-offs are addressed.

## 1. INTRODUCTION

Cellular metals exhibit property profiles that suggest their implementation as multifunctional materials [1-4]. The properties that appear most attractive are those that govern their use as cores for panels and shells having lower weight than competing materials and concepts. These advantages arise in certain ultra-light structures, in heat dissipation, for vibration control and for energy absorption. The benefits of cellular metals in such applications are topology-sensitive: that is, the important properties are sensitive to the micro-architecture of the cells. Establishing relationships between topology and performance represents the research frontier. This article explores the associated technical issues and discusses the research opportunities.

The known topological manifestations are either stochastic or periodic (figure1). The former represent commercially available closed and open cell alloy foams. The properties of such materials, as well as their implementation opportunities, have been comprehensively addressed in a recent book [1]. The most salient of these, summarized in the next section, establish performance benchmarks. The second comprises either regular

micro-truss architectures, referred to as lattice materials [5,6], or two-dimensional periodic channels, designated linear materials [7]. Such materials can be constructed with topologies exhibiting property profiles greatly superior to those demonstrated by their stochastic analogues, at the same relative density (or weight). However, fabrication costs are generally higher. Accordingly, it is important to quantify performance benefits and devise manufacturing cost models. Then, topological strategies that reduce weight may be created and implemented.

*The underlying concept is to design the topology of the structural alloy to carry load, conduct heat (and so on) in the most efficient manner (that is, at lowest weight): whereupon, the intervening space can be used to enable other functionalities, such as passages for flowing fluids that remove heat, spatially distributing plastic deformations that absorb energy, adding power sources, etc.*

The article is organized in the following manner. The relatively-well analyzed and documented thermo-mechanical performance characteristics of stochastic materials configured as cores in sandwich construction [1] are summarized. For this purpose, metrics have been chosen that allow the performance to be compared explicitly with competing concepts. Such results highlight implementation possibilities and provide benchmarks that direct opportunities for the development of lattice materials that might offer superior performance. These opportunities are discussed in section 3.

## 2 BENCHMARKS FOR PERFORMANCE

### 2.1 Ultra-light Structures

**Approach.** The measurements, models and analyses governing performance indices for metal foams are contained in [1,2,8-10]. These indices are used to create performance diagrams that highlight applications wherein foams offer advantages over competing concepts. For implementation as ultra-light sandwich construction, the shear modulus and strength of the foam material are the most important properties. These properties are related to those for the constituent alloy as follows. The shear modulus, G, is given by (figure 1b):

$$G / E_s \approx \alpha_{13}[1/2(1+\nu)]\rho^2 \qquad (1)$$

where $E_s$ is the Young's modulus of the constituent alloy, $\nu$ is the Poisson ratio of the foam ($\nu \approx 3/8$) and $\rho$ the relative density. The coefficient $\alpha_{13}$ is about unity for the best materials. The (factor 2) power law dependence on the relative density is indicative of ligaments that deform primarily in bending [2]. The shear yield strength $\tau_Y$ is given by:

$$\tau_Y / \sigma_Y^o \approx 0.3\beta_{13}\rho^{3/2} \qquad (2)$$

where $\sigma_Y^o$ is the yield strength of the constituent alloy. The coefficient $\beta_{13}$ is also about unity for the best materials. Again, the power law dependence on $\rho$ indicates a bending-dominated response. By using these basic properties in conjunction with the yield surface, sandwich configurations have been designed and compared with competing concepts. The performance indices required for this comparison include the yield strain for the alloy, $\varepsilon_Y$, as well as weight, load and stiffness indices. When the faces and the core are made from the same alloy, the weight index is [1,8]:

$$\Psi = W / LL_1^2\Omega_s \qquad (3)$$

where W is the overall structural weight, $\Omega_s$ the density of the alloy, L is the length of the panel (beam) and $L_1$ is either the radius of curvature (for cylinders) or the width (for panels). For designs based on load capacity, several indices have been used, but they are all interrelated. For axial compression, P per unit width, the most commonly used load index is:

$$\Pi_p = P / E_s LL_1 \qquad (4a)$$

An alternative index most suitable when the design involves face yielding is:

$$\Pi_p^* = P / \sigma_Y^o LL_1 \qquad (4b)$$

which is related to the other index by: $\Pi_p = \Pi_p^* \varepsilon_Y^0$, with $\varepsilon_Y^0$ being the yield strain for the alloy. For bending, the index most frequently used is:

$$\Pi_b = V / \sqrt{E_s M} \qquad (4c)$$

where M is the moment and V the shear force, both per unit width. This index is related to that in compression by: $\Pi_b = \Pi_e^2$. For stiffness limited designs in structures subject to bending, the preferred index is:

$$\Im = P / \bar{\delta} E_s \qquad (5)$$

where $\bar{\delta}$ is the allowable displacement.

**Minimum weight designs** are found by identifying the failure modes, specifying the stiffness or load capacity and then varying the dimensions to determine the lowest weight for each failure mode. The constraints cause the design to reside within one of these domains: whereupon an optimum can be found. For foam core sandwich configurations, the operative failure modes (figure 2) comprise core shear, face yielding and core indentation (the face wrinkling and interface debonding mechanisms found in panels made from other materials appear to be unimportant in cellular metal construction). A representative example of how failure modes that govern the minimum weight change as the ratio of face thickness to loading span, t/L, changes is depicted on figure 2. In all of the following results, implicit to each minimum weight design are specific values for the core and face sheet thickness, identified through formulae presented in [1].

When **load capacity** governs the design, the general finding is that, for flat panels subject to bending, foam core sandwich construction is not competitive on a performance basis; honeycomb core panels are always lighter for the same performance (figure 3). Nevertheless, implementation opportunities still exist, based on cost, durability and other performance criteria, such as strength retention after impact. But these need further assessment. *Conversely, explicit performance benefits have been ascertained for non-planar foam core configurations* (such as curved panels, shells and box beams). This happens because the isotropy of the foams (relative to honeycombs), combined with the bi-axial nature of the induced strains, lend themselves to lower weights than either honeycomb-core or stringer stiffened panels. Examples for designs requiring that specified loads be supported at minimum weight (figure 4) illustrate the benefits. In such cases, foam core sandwich construction is preferred for shells, as well as box beams, in either compression or bending. The weight savings for an alloy with $\varepsilon_Y \approx 0.007$ (representative of high strength Al

alloys), summarized on figure 4, can be as large as 50%. These reduced weights exist at moderate and low levels of the load index, because the load capacity is wrinkling-dominated and the core resists this failure mode. At larger loads, the load capacity is dominated by yielding, whereupon the core provides no support and the benefits are lost. Note that the weight benefits arise at low levels of relative density (0.05 to 0.1), subject to the premise that (1) and (2) still apply. Finally, for axially compressed flat panels, while hat-stiffening is more efficient than foam core sandwich construction, when foam cores are introduced into the stiffeners the overall configuration is even lighter (figure 5).

When designs are **stiffness-limited**, the opportunities for weight savings are configuration and loading specific. To illustrate the characteristics, the minimum weights of flat panels subject to distributed (pressure) loads have been calculated as a function of load index at various foam densities, at an allowable displacement, $\bar{\delta} = 0.01L$ (figure 6). These results reveal that the stiffness (rather than strength) is most likely to govern the weight at smaller load indices. Moreover, in this range, the minimum weight decreases as the core density decreases, subject to (1) and (2) still having applicability.

### 2.2 Heat Dissipation Media

Open cell metals constitute a medium for efficient heat transfer. The specifics are manifest in cross plots of heat dissipation and pressure drop indices [1,9] (figure 7). These indices are derived by modeling the temperatures and the pressure drops as variants on those expected for a bank of cylinders with unknown numerical coefficients that reflect the non-uniform topology [9,10]. By measuring these coefficients for several commercial foams, and upon assuming that the same coefficients are applicable over a wide range of relative density and cell size, performance maps (figure 7) have been calculated. Note that, because so many parameters are involved, these maps have been constructed for specific (albeit realistic) choices for the fluid flow rate and core thickness. The "preferred" material domain is circled at the lower left. It refers to materials

that have excellent heat dissipation characteristics at acceptably-low pressure drop. These materials have cell diameter, $d$, in the millimeter range and relative densities of order: $\rho \approx 0.2$. The rationale for explicit determination of the preferred characteristics is described next. Note that the preferred densities exceed those that give rise to minimum weight sandwich construction (figure 5).

Specific preferences are found by invoking categories of fluid pumps and overlaying their characteristics with those for the cellular metal. An illustration is shown on figure 8 [1]. Pumping systems have flow velocities $\dot{V}$ (in liters/s) that diminish with increase in pressure drop, $\Delta p$, in an approximately linear manner. Conversely, the cellular medium exhibits a pressure drop that increases with increase in $\dot{V}$. Accordingly, the combined system operates at the intersection, characterized by specific flow rate, $\dot{V}_*$, and associated pressure drop. Based on this flow rate and its dependence on cell topology, the heat dissipation can be determined as functions of $\rho$ and $d$ for a pumping device having specified back pressure. The results (figure 8) indicate an optimum cell size in the mm range with a weak dependence on the relative density. Using this basic approach, the attributes of the cellular metal can be assessed on a case-by-case basis. Often, substantial improvements in compactness can be achieved relative to competing concepts.

### 2.3 Other Functionalities

Cellular metals have the **highest energy absorption** per unit mass of any material [1]. Their characteristics are summarized on figure 9, where they are compared with a theoretical upper bound for tubes. They are effective because of the interplay between intense plastic work (enabled by the cellular structure) and the relatively low pressure at which the absorption takes place. While tubes might be somewhat superior to the cellular material for a unidirectional impact, the isotropy of the foam is advantageous for impacts from unanticipated directions. Moreover, foam filled tubes have synergistic energy absorption, relative to empty tubes and

cellular material alone (figure 10), because the foam interior diminishes the buckling wavelength in the tube.

Sandwich panels made with cellular metal cores have **high natural vibration frequencies** because of their large bending stiffness per unit mass [1]. The lowest frequency, $\omega$, for a circular plate, radius R, thickness, H, scales as:

$$\omega \sim [E_s \rho^2 H^3 / mR^4]^{1/2} \qquad (6)$$

with m being the mass. Since, at constant mass, the thickness is inversely dependent on $\rho$, the net trend is a frequency that scales as: $\omega \sim \rho^{-1/2}$. That is, the vibration frequency can be increased beyond the resonances by fabricating panels with a sufficiently low core density.

The ductile nature of metal core panels enables their strength in bending and compression to be **insensitive to degradation by impact**. This robust response contrasts with the sensitivity of composite panels to strength degradation upon impact.

## 3. PERIODIC MATERIALS

### 3.1 Structural Characteristics

***(i) Lattice Materials***

Two categories of lattice material have been subject to measurement and analysis. One has been referred to as lattice block (LBM) material [5]. Another, configured with nodes in a face-center tetragonal arrangement has been designated the octet truss material (OTM) [6,11]. In both cases, the lattices are designed such that the trusses are in tension/compression with no bending. The absence of bending allows the stiffness and strength to vary linearly with relative density [5,6]:

$$G_{ij} / E_s = A_{ij} \rho \qquad (7a)$$

$$\tau_{ij} / \sigma_Y^o = B_{ij} \rho \qquad (7b)$$

with the coefficients $A_{ij}$ and $B_{ij}$ being functions of truss architecture and loading orientation, $\theta$. A single layer OTM (configured as a core bonded to a dense face layer) is almost isotropic. When constructed with “rigid”

nodes, the coefficients in (7) are: $A_{13} = A_{23} = 1/9$, $B_{13} = 1/3\sqrt{2}$ [6,12]. Note, however, that for minimum weight designs, (7b) does not represent the salient shear characteristic, because the response is dictated by elastic buckling of the compressed trusses in the core [6]. Comparisons with (1) and (2) indicate that, at a relative density, $\rho \approx 0.1$, this material is about 3 times stiffer than the best open cell foam and has greater strength by a similar factor. These superior properties are reflected in weight savings, elaborated below. The lattice block materials are anisotropic [5]. Their in-plane shear stiffness' are plotted on figure 11a as a function of the cell aspect ratio. The highest values correspond to $A_{13} \approx 0.05$. These stiffness maxima are slightly higher than those for the stochastic materials in the most relevant density range ($\rho \leq 0.2$), but only about half that for the octet truss. Corresponding values of the in-plane shear strength are plotted on figure 11b. Again the maximum strengths are lower than those for the octet truss material, but exceed those for the best stochastic materials.

The properties of these materials have yet to subject to the level of experimental validation needed to justify implementation. Defects that degrade the properties are to be expected. While it remains to determine how important these are, measurements of stiffness and strengths of Al alloy lattice block materials [5] imply that the knock-down factors could be relatively small.

***(ii) Linear Materials***

Linear materials have periodic, open channels that extend the length of the structure in accordance with a variety of cross sectional topologies (figure 12). From a structural perspective, as cores within sandwich construction, the triangular topology is much superior to all other possibilities [13]. It is the only one that enables the trusses to be in tension or compression (that is, no bending) when subject to in-plane shear. Accordingly, it has a linear dependence on $\rho$, in accordance with (7a), with: $A_{13} = 1/8$ (Appendix). In all other cases, the scaling is: $G \sim \rho^3$ (Appendix). Hence, strictly on a structural basis, the triangulated material is vastly superior to all others and slightly

better than the OTM lattice. Other topologies become worthy of consideration when thermal performance dominates, as elaborated below.

***(iii) Performance Benefits***

Full optimizations have been conducted for single-layer, OTM core sandwich panels, based on load capacity [6]. These have been used to ascertain the minimum weights of flat panels subject to bending (figure 3) and compression (figure 5b). The general finding is that the truss core panels are about as lightweight as the most efficient, competing sandwich construction: namely, honeycomb core panels (bending) or hat-stiffened panels (compression). When cooling and other functionalities are incorporated, the lattice materials become even more attractive than the alternative concepts, as addressed next.

### 3.2. Heat Dissipation and Bi-functionality

Analyses of the heat dissipation achievable with linear materials when subject to forced air convection, in a dynamic range characterized by laminar flow [12], provide insights (figure 12). The results have been expressed in terms of a non-dimensional index that captures the interplay between heat transfer coefficient $\bar{h}$ and pressure drop $\Delta p$. This index is given as:

$$I_1 = [\nu_F \Omega_F u / k_s]\bar{h} / \Delta p \qquad (8)$$

where u is the fluid velocity, $k_s$ the thermal conductivity of the solid, $\nu_F$ the kinematic viscosity and $\Omega_F$ the density of the fluid. Evidently, the larger this index, the greater the heat dissipation at fixed pumping power. For each cell, when the core thickness is specified, this index exhibits a maximum, $I_1^{\max}$ with an associated relative density. Accordingly, for each cell, there is a unique relation between the structural weight per unit cross section and the peak heat dissipation capacity at specified pumping power. This dependence is plotted on figure 13. Evidently, cells with hexagonal cross section enable heat dissipation at lowest weight and, moreover, are the only topology capable of adequate dissipation at the highest heat fluxes. Corresponding results for lattice materials have yet to be derived. Although,

initial simulations indicate that they will exhibit heat dissipations at specified pressure drop superior to, open cell foams.

Designs that combine structural load capacity with heat dissipation bring into focus a topological dichotomy: namely, triangles provide the best structural characteristics and hexagons the worst, whereas for heat dissipation the ranking is the opposite. To explore this interplay, the product of $I_1^{\max}$ with $G/E_s$ has been chosen as a new index, denoted $\hat{I}_2$. The index only has relevance for specified core thickness, H, relative to cell size, $l$. Accordingly, plots of the structural weight as a function of this index, for two choices of $H/l$ (figure 14), provide useful insights.

The implications depend on the levels of heat flux that impinge on the panel. When the heat flux is relatively low so that relatively thin cores can be used, which are compatible with minimum weight structural designs (figures 3 to 5), the lowest overall weight for combined load bearing and heat dissipation is achieved with the triangular cell material. Conversely, when the application is dominated by heat dissipation requirements, requiring a thicker core, hexagonal cells seem to be preferred.

## 4. MANUFACTURING

Stochastic materials are manufactured by foaming, which is used either to create the metal directly (closed cell) or to form a template (open cell) [1]. Images of some stochastic materials are shown on figure 15. There are three variants for closed cell materials. (i) The coalescence of bubbles, with subsequent drainage to thin the ligaments and membranes (figure 16a), generates materials with large cells, centimeters in diameter [14]. (ii) The decomposition of $TiH_2$ particles in liquid aluminum creates similar materials, Figure 16b, but with a smaller cell size and more controllable relative density [15]. (iii) Powder metallurgy methods can also be used, Figure 16c, because $TiH_2$ decomposes rapidly well below the melting temperature of most aluminum alloys [16]. Processes (ii) and (iii) allow the manufacture of near net shape parts, but lower relative densities are achievable with process (i), because of drainage. Open cell materials are

made by commencing with a reticulated polymer foam as a template. In commercial practice, a metal version of the structure is created by investment casting and pressure infiltration (figure 17). Alternatively, either a fine metal slurry can be coated onto the polymer and sintered [17], or a metal vapor deposited and the ligaments densified by transient liquid phase sintering [18].

Lattice materials are made by one of three processes. (i) Injection molding is used to create a polymer template of the lattice structure, with/without face-sheets, followed by investment casting [19]. This process appears to be limited to cells in the centimeter size range, negating their cooling functionality. (ii) Alternatively, fabricating the template by rapid prototyping (figure 18) enables materials with smaller cells to be made (in the millimeter range), as well as allowing position dependent control of the placement of the polymer, whereupon the structure can be graded. (iii) A textile analogue may be used to create a metal mesh, Figure 19, which is stacked, laminated and bonded at the nodes by either diffusion bonding or liquid phase sintering [20]. Face-sheets are attached by similar processes.

## 5. CONCLUSIONS

Methods have been developed to create cellular metals with a wide range of topologies. Stochastic materials are inexpensive but place material in locations where it contributes little to material properties (other than density). Periodic materials can be made by several (for the most part) expensive techniques. They can be designed to optimize multifunctionality by placing material at locations where mechanical and other performance indices are simultaneously maximized. Inexpensive manufacturing methods that enable control of the topology are needed.

## APPENDIX

**Shear Moduli For Linear Materials** [2, 12].

The in-plane shear modulus of an array of square cells with connectivity 4 is

$$G / E_s = (1/2)(t/l)^3 \qquad \text{(A1a)}$$

For square cells with connectivity 3,

$$G / E_s = (4/5)(t/l)^3 \qquad \text{(A1b)}$$

For regular hexagonal cells,

$$G / E_s = (1/\sqrt{3})(t/l)^3 \qquad \text{(A1c)}$$

For triangular cells with connectivity 4,

$$G / E_s = 89(t/l)^3 \qquad \text{(A1d)}$$

and, for triangular cells with connectivity 6,

$$G / E_s = (\sqrt{3}/4)(t/l) \qquad \text{(A1f)}$$

where

$$t / l = c_t(1 - \sqrt{1-\rho}) \qquad \text{(A2)}$$

with $c_t = 1,\ 0.577,\ 1.732$ for square, triangular and hexagonal cells, respectively.

## REFERENCES


1. M.F. Ashby, A.G. Evans, N.A. Fleck, L.J. Gibson, J.W. Hutchinson, H.G.N. Wadley, *Metal Foams: a Design Guide*, Butterworth-Heinemann, June, 2000.
2. L.J. Gibson, M.F. Ashby, *Cellular Solids: Structure and Properties*. (2nd Edition), Cambridge University Press, 1997.
3. A.G. Evans, J.W. Hutchinson, M.F. Ashby, *Progress Mtls. Sci*., **43**, 171-221 (1998).
4. J. Banhart, M.F.Ashby, N.A.Fleck, *International Conference on Metal Foams and Porous Metal Structures*, 14th - 16th, Bremen (Germany) (June 1999).
5. J.C.Wallach, L.G. Gibson, Mechanical Behavior of a Three-Dimensional Truss Material (2000). Submitted to *Int. J. Solids and Structures.*
6. N.Wicks, J.W.Hutchinson, *Optimal Truss Plates*, (March 2000) to be published.
7. J. Cochran, *unpublished research*
8. B. Budiansky, *Int. J. Solids Struc*., **36,** 3677 - 3708 (1999).
9. A.Bastawros, H. A. Stone and A.G.Evans, *Jnl Heat Transfer*, in press
10. T.J.Lu, H.A.Stone and M.F.Ashby, *Acta Mater.*, **46**, 3619-3635 (1998).
11. R. B. Fuller, U.S.Patent, 2,986,241 (1961).
12. V. Deshpande and N.A. Fleck, *unpublished research.*
13 S.Gu, T.J.Lu and A.G.Evans, *Intl Jnl Heat Transfer*, to be published.
14. J.T. Wood, "Metal Foams" Editors: J. Barnhart and H. Eifert, MIT Verlag Publishing (Bremen), 1998, 31-38.
15. T. Miyoshi, M. Itoh, S. Akiyama, and A Kitahara, "Porous and Cellular Materials for Structural Applications". Editors: D.S. Schwartz, D.S. Shih, A.G. Evans, and H.N.G. Wadley, MRS Symposium Proceedings VOL 521, MRS (Warrendale), 1998, 133-137.
16. C-J. Yu and H. Eifert, *Advanced Materials and Processes*, 1998, 45-47.
17. J. Banhart and J. Baumeister, "Porous and Cellular Materials for Structural Applications", Editors: D.S. Schwartz, D.S. Shih, A.G. Evans, and H.N.G. Wadley, MRS Symposium Proceedings VOL 521, MRS (Warrendale), 1998, 121-132.
18. D.T. Quihellalt, D.D. Hass, D.J. Sypeck, P.A. Parrish, and H.N.G. Wadley, *Materials Science and Engineering*, Submitted, 2000.
19. N.A. Fleck, *Private Communication*, 2000.
20. D. Sypeck and H.N.G. Wadley, *In preparation*.

**FIGURE CAPTIONS**

Figure 1a A schematic illustrating the two predominant topologies exhibited by cellular metals.

Figure 1b. A comparison of the elastic moduli measured on stochastic closed cell Al alloys with those for FCC lattice materials.

Figure 2. The failure modes exhibited by sandwich panels in bending and an illustration (bottom) of how the failure loci change with the face and core thickness. Also shown is the minimum weight design for a panel with an allowable deflection $\bar{\delta} / l = 0.01$ at a load index, $\Pi = 10^{-4}$.

Figure 3. The minimum weights as a function of collapse load for panels subject to edge loads P: a comparison of four competing core configurations.

Figure 4. Minimum weights for axially compressed configurations as a function of load index. (a) Box beams showing that an annular design has lowest weight. Similar results apply in bending. (b) Shells showing that sandwich configurations have lower weight than axially stiffened designs.

Figure 5. Minimum weights of compression panels showing that sandwich construction made with stochastic core materials are not competitive with hat stiffened panels: whereas truss core panels and hat–stiffened sandwiches have lower weights, especially at lower levels of load index.

Figure 6. Weight index as a function of load index for optimally designed Al alloy sandwich panels subject to an allowable displacement ($\bar{\delta} / l$ = 0.01). Note that the design is deflection limited at small values of the load index, but becomes strength limited at larger values.

Figure 7. Considerations relevant to the use of open cell materials as heat dissipation media. The materials are effective because of a combination of efficient conduction into the medium along the conductive ligaments with a high internal surface area for effective heat transfer into the fluid. The cross plot of heat dissipation against pressure drop suggests that the preferred material is one having a cell size in the mm range and a relative density of

order 0.2. ($\tilde{d}$ is the non-dimensional ligament diameter, Re is the Reynolds number, Pr the Prandtl number and $k_f$ the thermal conductivity of the fluid.

Figure 8. An illustration of the thermal performance achievable using open cell metal heat sinks. (a) The pressure drop against flow rate characteristics of the heat sink and the pumping system showing that for each configuration there is a representative flow rate, $\dot{V}_*$, at the intersection of the the curves. (b) For each cellular material, based on trends in $\dot{V}_*$, a specific level of heat dissipation, q, can be achieved upon using a pump with given operating characteristics. The plot of q against relative density and ligament diameter reveals that the peak levels achievable coincide with cells in the mm size range.

Figure 9. The energy absorbed per unit mass by tubes (full line) and by metal foams, plotted against the plateau stress. The data for tubes derive from and upper bound calculation of the collapse stress. Each foam is labeled with its density in $Mg/m^3$.

Figure 10. Crushing force as a function of axial compression for open tubes, foam and foam-filled tubes. The plot (1) +(2) refers to expectations from the tests on open tubes and foam separately. That the actual results for the filled tubes exceed this indicate a synergistic effect caused by a decrease in the buckling wavelength enabled by the foam core.

Figure 11 A comparison of some of the mechanical properties of lattice block and FCC lattice materials. (a) In-plane shear modulus and (b) in-plane shear strength.

Figure 12. Linear material core configurations.

Figure 13. The structural weight as a function of the peak heat dissipation capacity, $I_1$ (defined in (8)) for each of the cells depicted on figure 12. Note the superior performance of the hexagonal cells.

Figure 14. Structural weight as a function of the thermo-mechanical performance index. These plots reveal that for panels with thin cores subject to low heat flux, triangular materials yield lowest weight: whereas in high heat flux scenarios, requiring thicker cores, hexagons are the lightest.

Figure 15 Images of stochastic materials made by a variety of manufacturing processes.

Figure 16a A gas injection process creates closed cell, stochastic aluminum foam. Small SiC particles are incorporated to impede drainage and strengthen cell membranes to avoid premature rupture during foaming.

Figure 16b Titanium hydride particles are dispersed in molten aluminum alloys to create closed cell materials. Calcium is often added to increase the melt viscosity (slow the drainage).

Figure 16c Powder metallurgy methods are also used to disperse titanium hydride in aluminum powder. The powder is consolidated and upon heating above 550C undergoes foaming.

Figure 17 Open cell reticulated polymer foams are used as templates for investment casting. After removal of the polymer, liquid metal is introduced and solidified.

Figure 18 Polymer octet truss structures made by rapid prototyping are used as templates for investment casting.

Figure 19a. Woven structural alloy wires are used to create a micro-truss lay-up. Transient liquid phase sintering of the nodes creates a periodic material with or without face-sheets.

Figure 19b Example of a woven micro-truss material made from Nichrome.

# TWO CATEGORIES OF CELLULAR METAL

**I** **Stochastic**

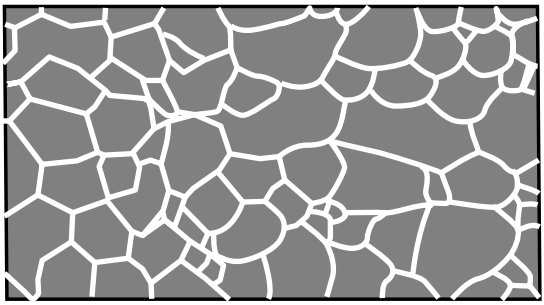

**II** **Periodic**

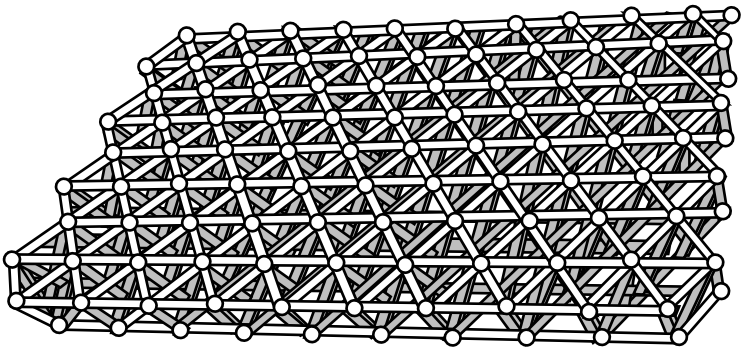

Figure 1A

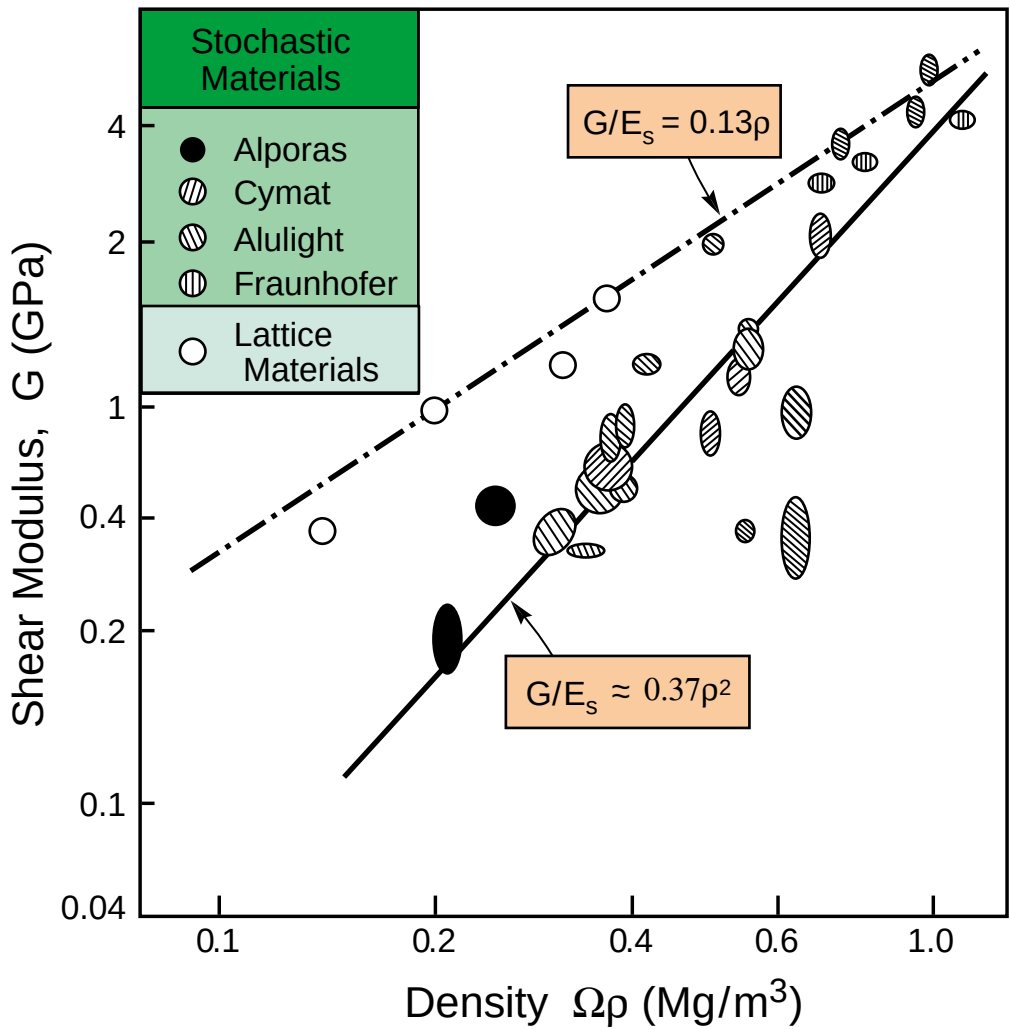
CELLULAR Aℓ STIFFNESS
Stochastic Materials
Alporas
Cymat
Alulight
Fraunhofer
Lattice Materials
G/E_s = 0.13ρ
G/E_s ≈ 0.37ρ²
Shear Modulus, G (GPa)
4
2
1
0.4
0.2
0.1
0.04
0.1
0.2
0.4
0.6
1.0
Density Ωρ (Mg/m³)

Figure 1B

# WEIGHT MINIMIZATION

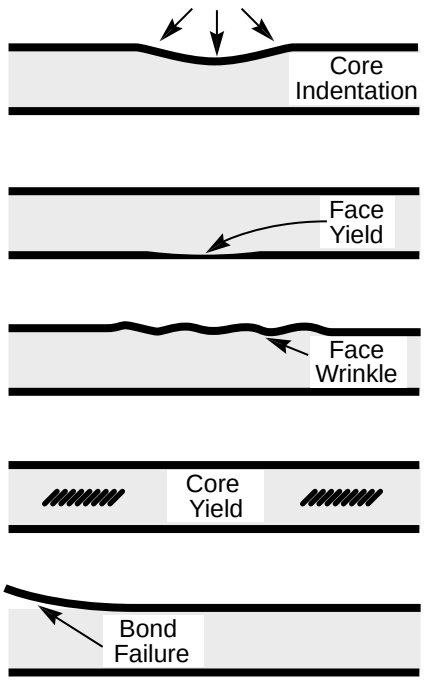


Failure Modes

Loading

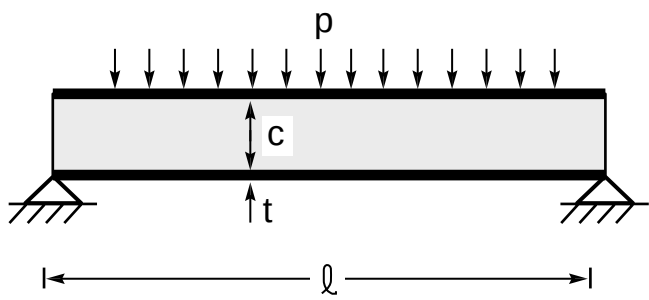


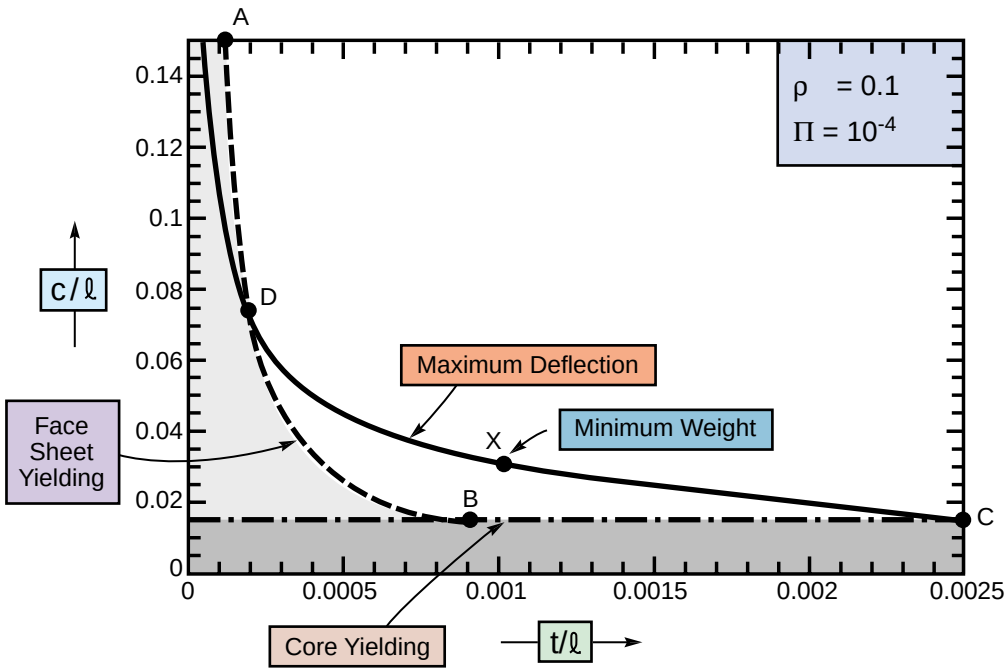


Figure 2

# PLATE BENDING COMPARISON

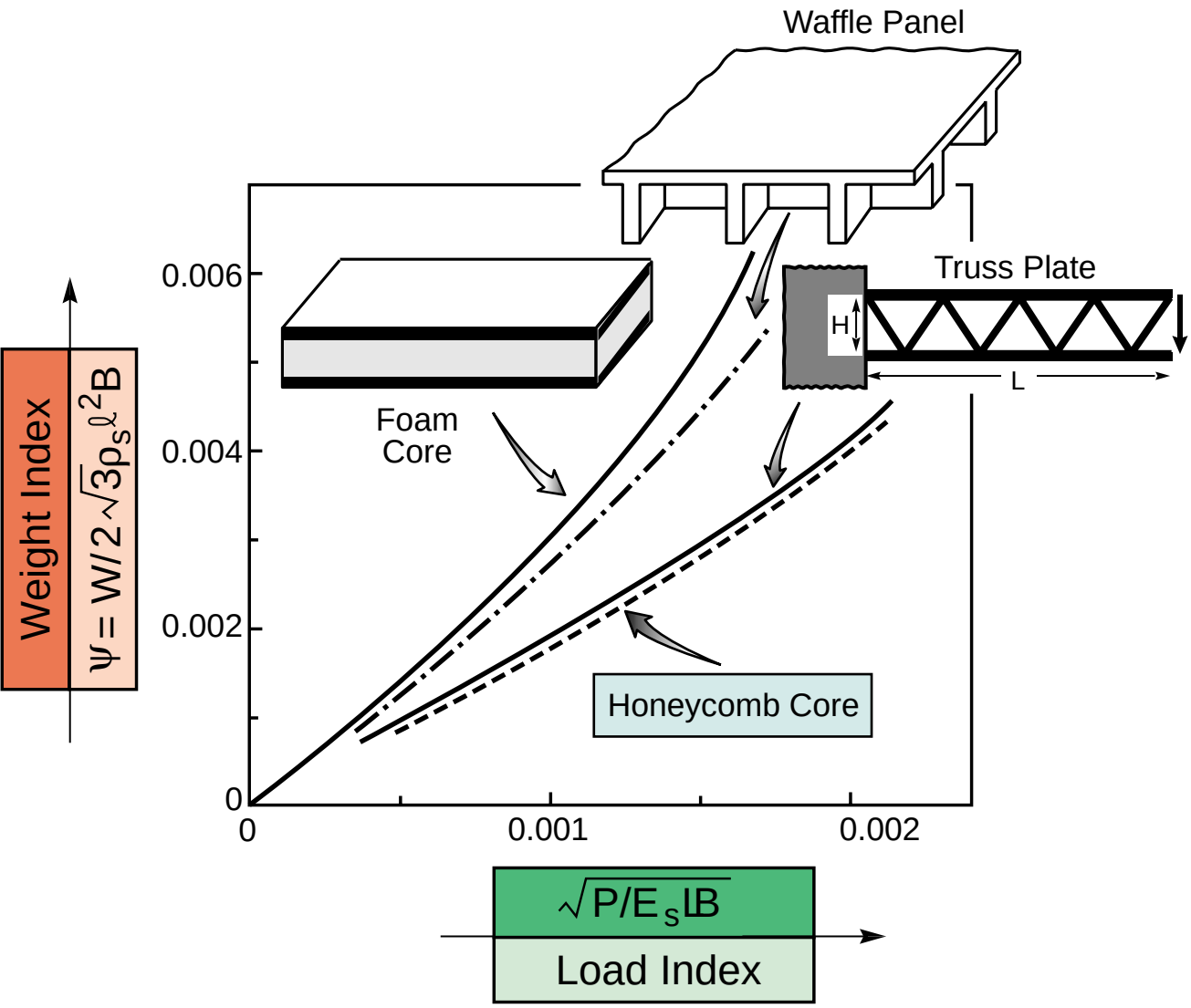


Figure 3

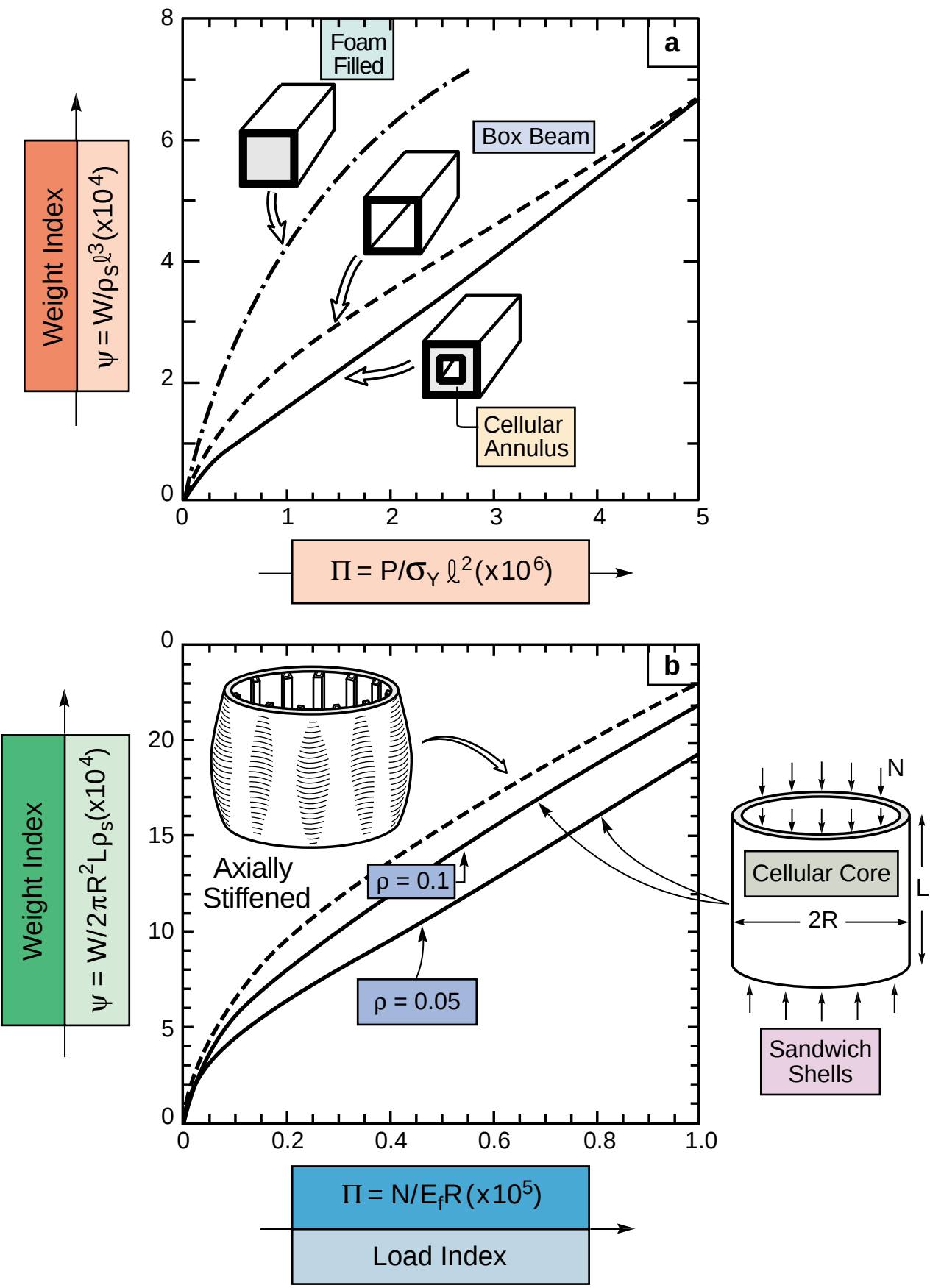
a
Foam Filled
Box Beam
Cellular Annulus
Weight Index
$\psi = W/\rho_s \ell^3 (x10^4)$
$\Pi = P/\sigma_Y \ell^2 (x10^6)$
b
Axially Stiffened
ρ = 0.1
ρ = 0.05
N
Cellular Core
2R
L
Sandwich Shells
Weight Index
$\psi = W/2\pi R^2 L \rho_s (x10^4)$
$\Pi = N/E_f R (x10^5)$
Load Index

Figure 4

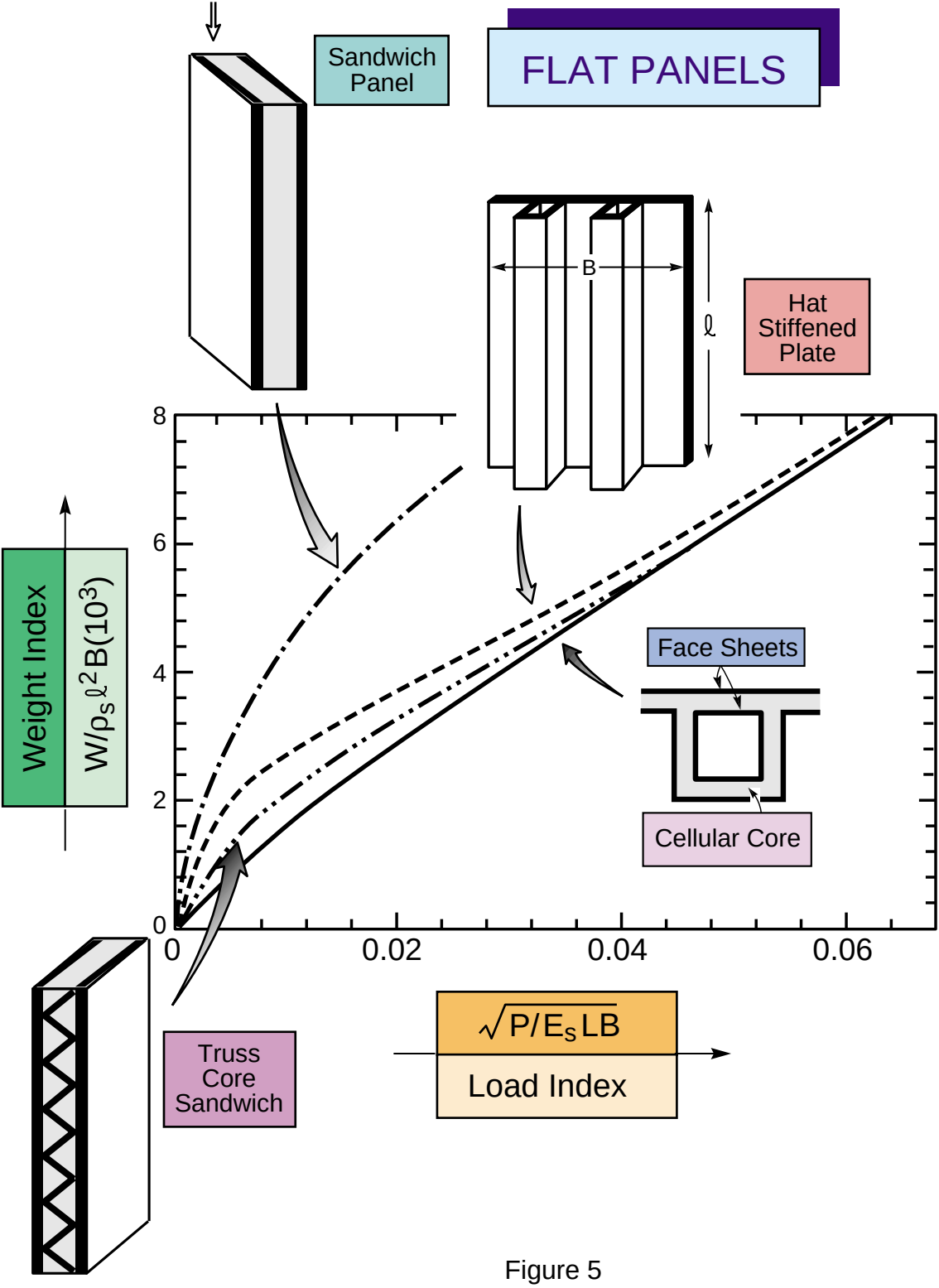
FLAT PANELS
Sandwich Panel
B
ℓ
Hat Stiffened Plate
Face Sheets
Cellular Core
Weight Index
$W/\rho_s \ell^2 B(10^3)$
8
6
4
2
0
0
0.02
0.04
0.06
$\sqrt{P/E_s LB}$
Load Index
Truss Core Sandwich

Figure 5

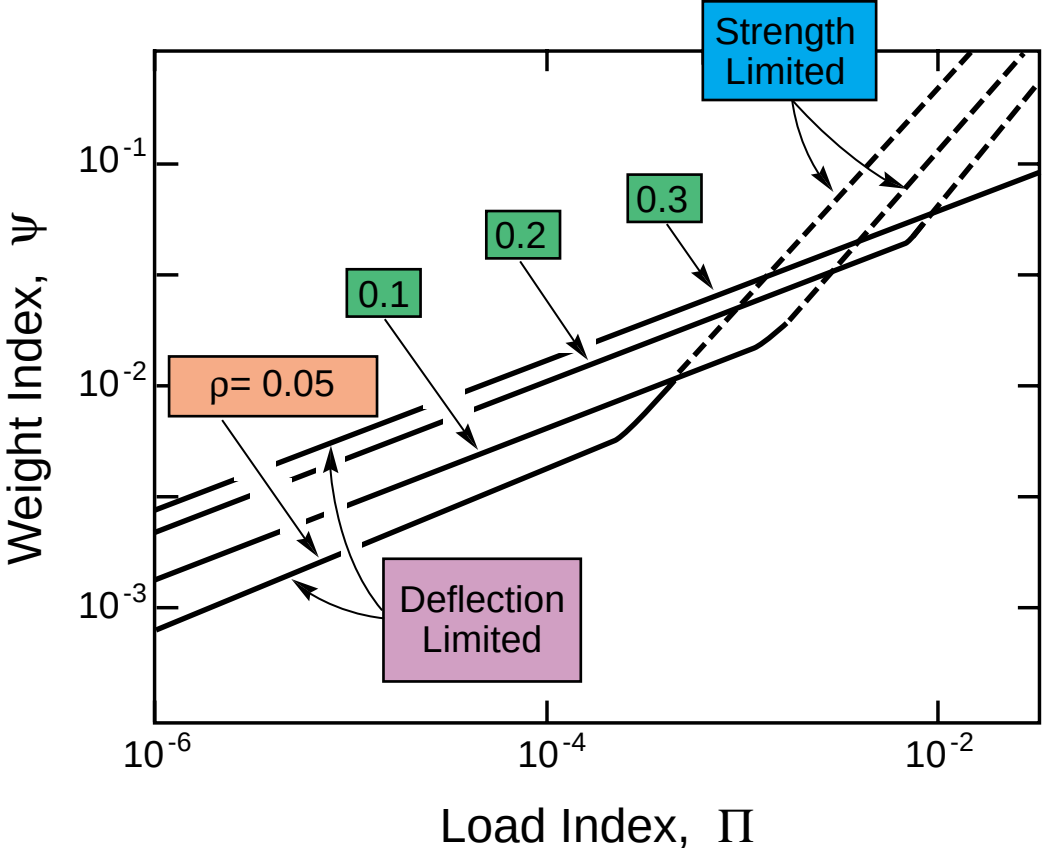
Strength
Limited
0.3
0.2
0.1
ρ= 0.05
Deflection
Limited
Weight Index, ψ
Load Index, Π
10-1
10-2
10-3
10-6
10-4
10-2

Fig. 6

# CELLULAR HEAT TRANSFER MEDIUM

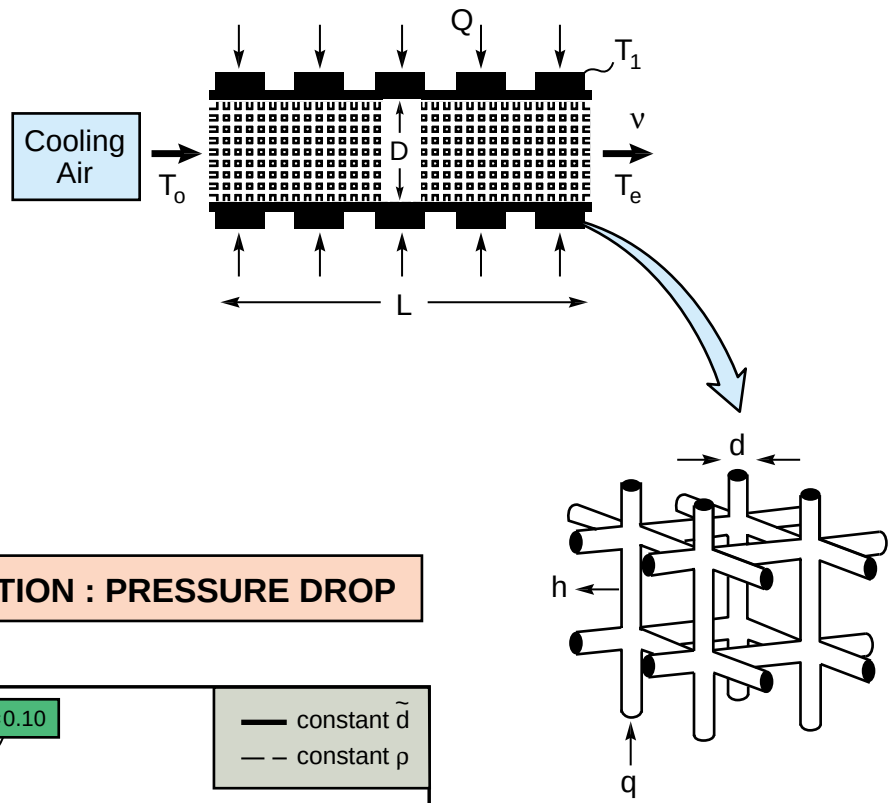


## HEAT DISSIPATION : PRESSURE DROP

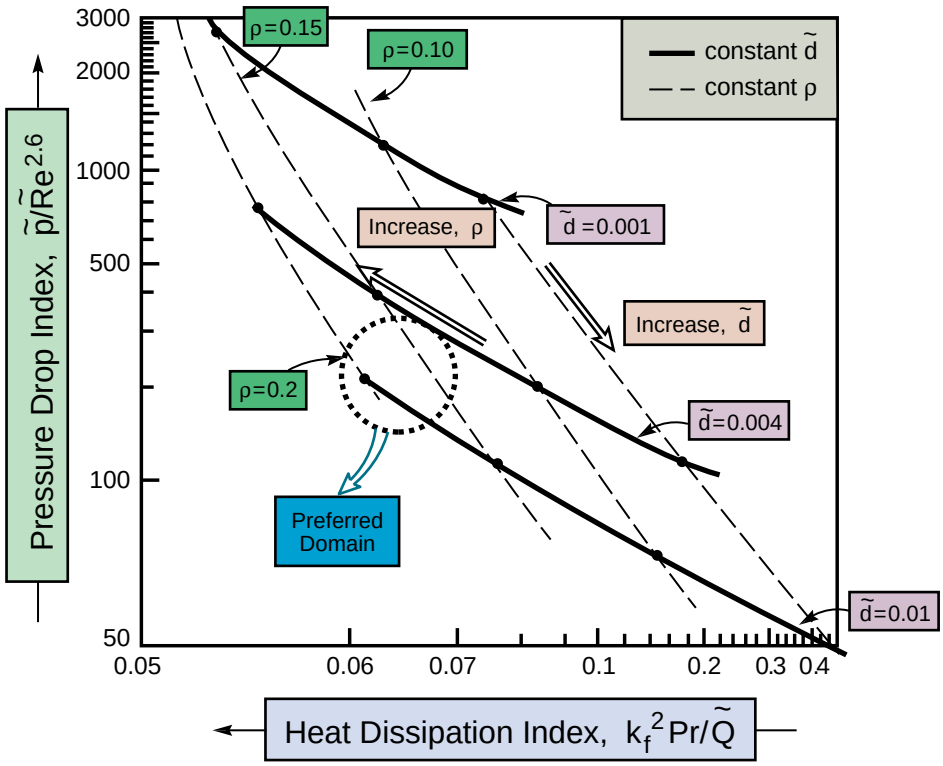


Figure 7

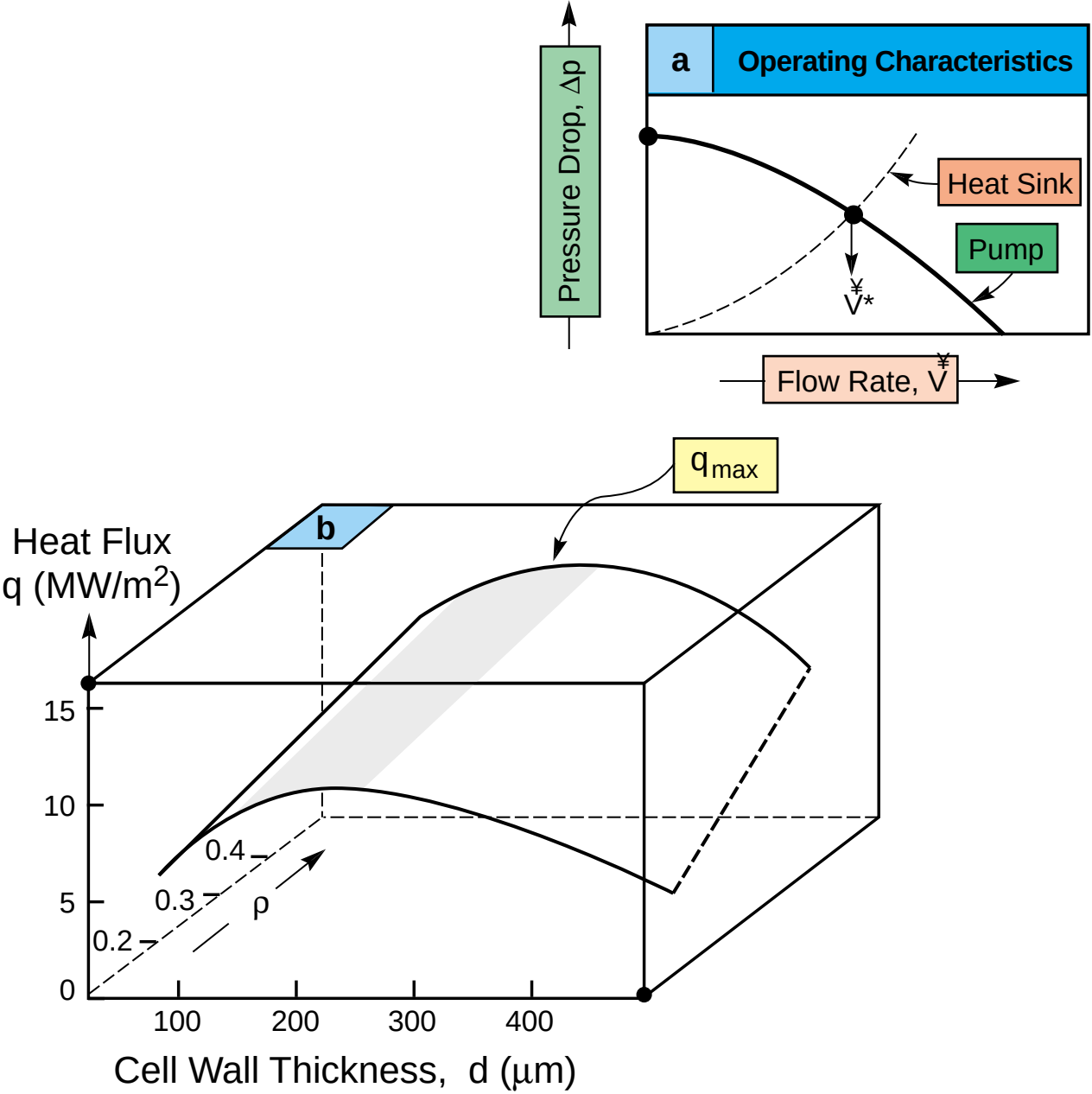
a
Operating Characteristics
Pressure Drop, Δp
Heat Sink
Pump
V̄*
Flow Rate, V̄
b
q_max
Heat Flux
q (MW/m²)
15
10
5
0
0.4
0.3
0.2
ρ
100
200
300
400
Cell Wall Thickness, d (μm)

Fig. 8

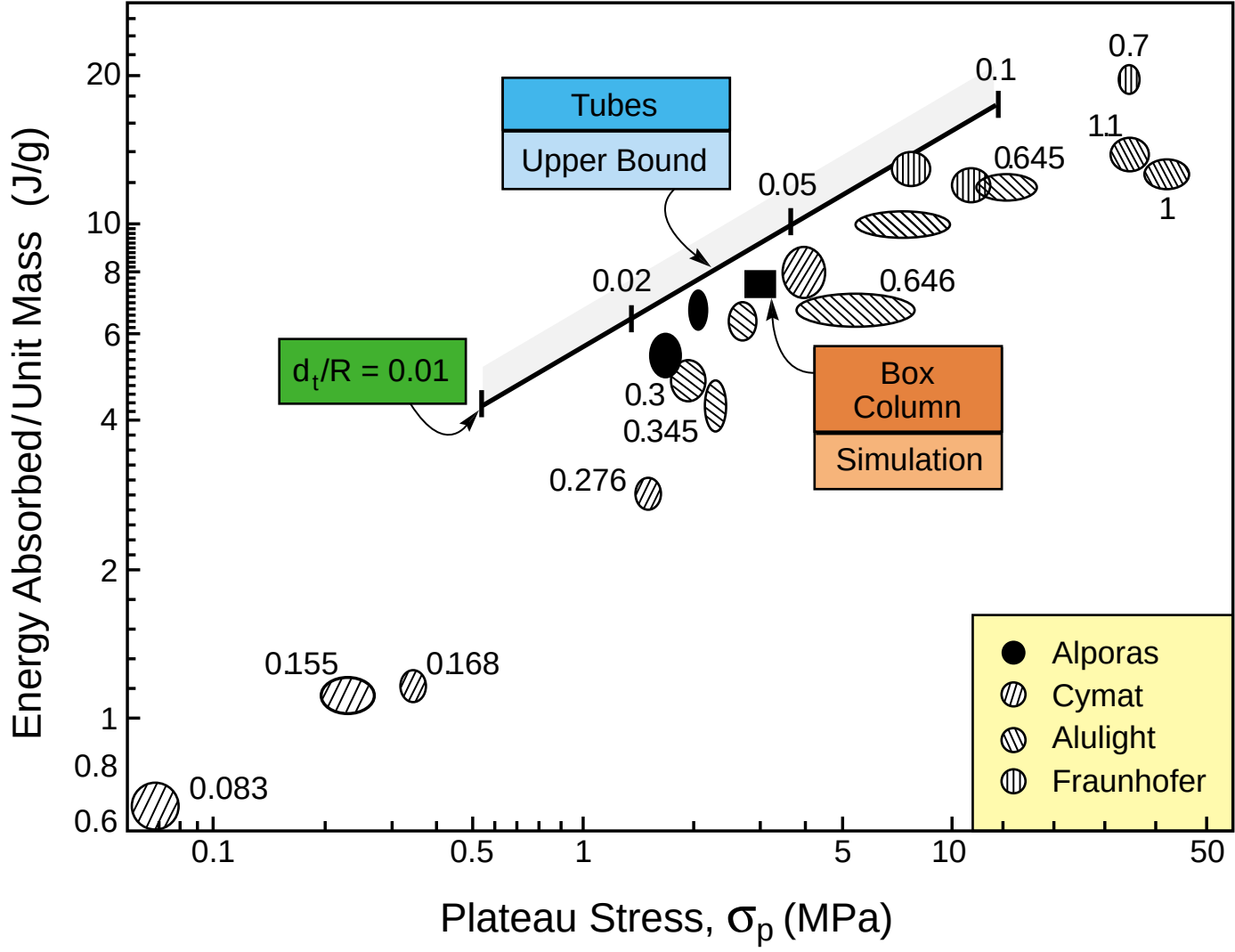
Energy Absorbed/Unit Mass (J/g)
20
10
8
6
4
2
1
0.8
0.6
0.1
0.5
1
5
10
50
Plateau Stress, σp (MPa)
Tubes
Upper Bound
dt/R = 0.01
Box
Column
Simulation
0.1
0.05
0.02
0.7
1.1
1
0.645
0.646
0.3
0.345
0.276
0.155
0.168
0.083
Alporas
Cymat
Alulight
Fraunhofer

Fig. 9

# ENERGY ABSORPTION

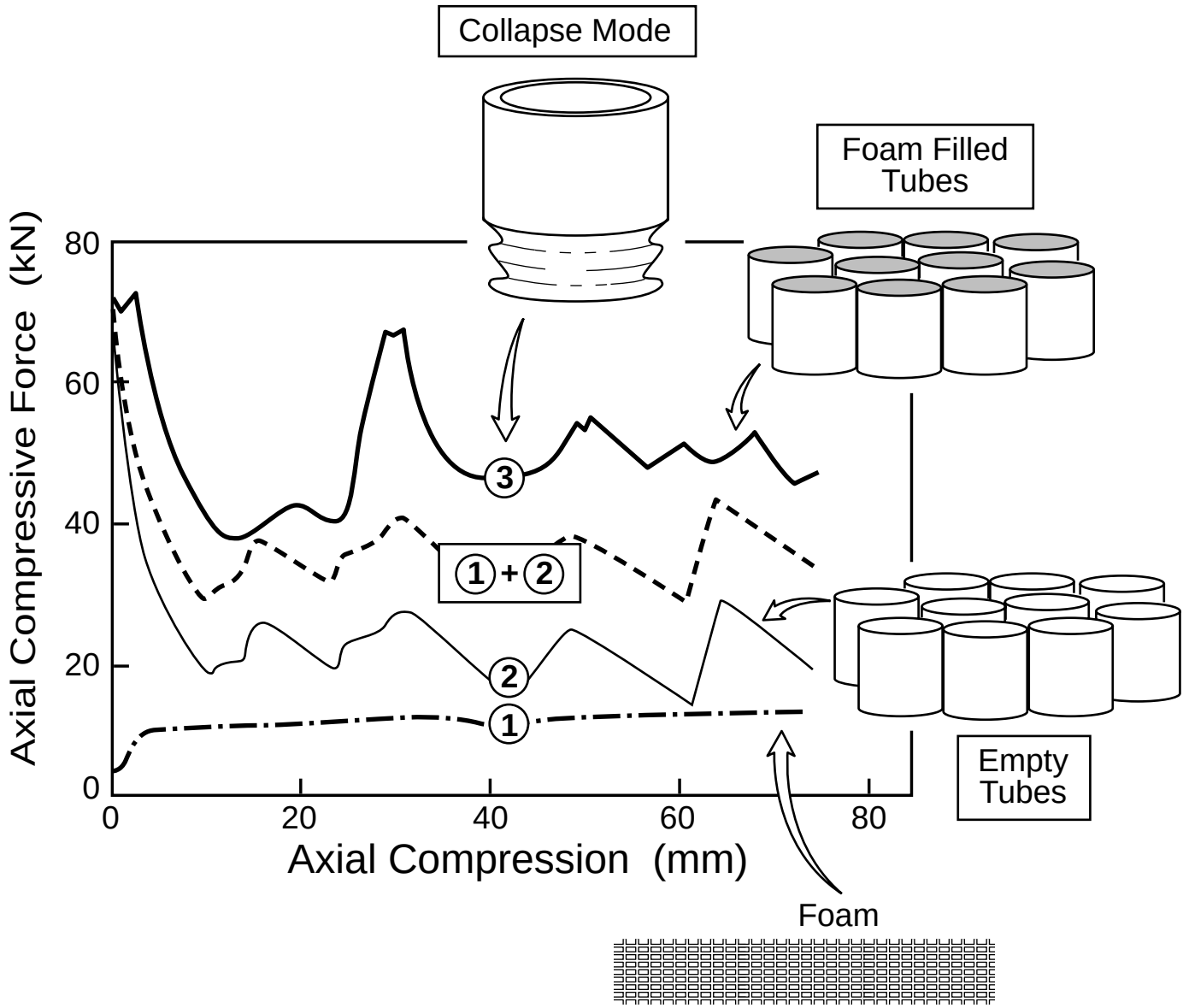


Figure 10

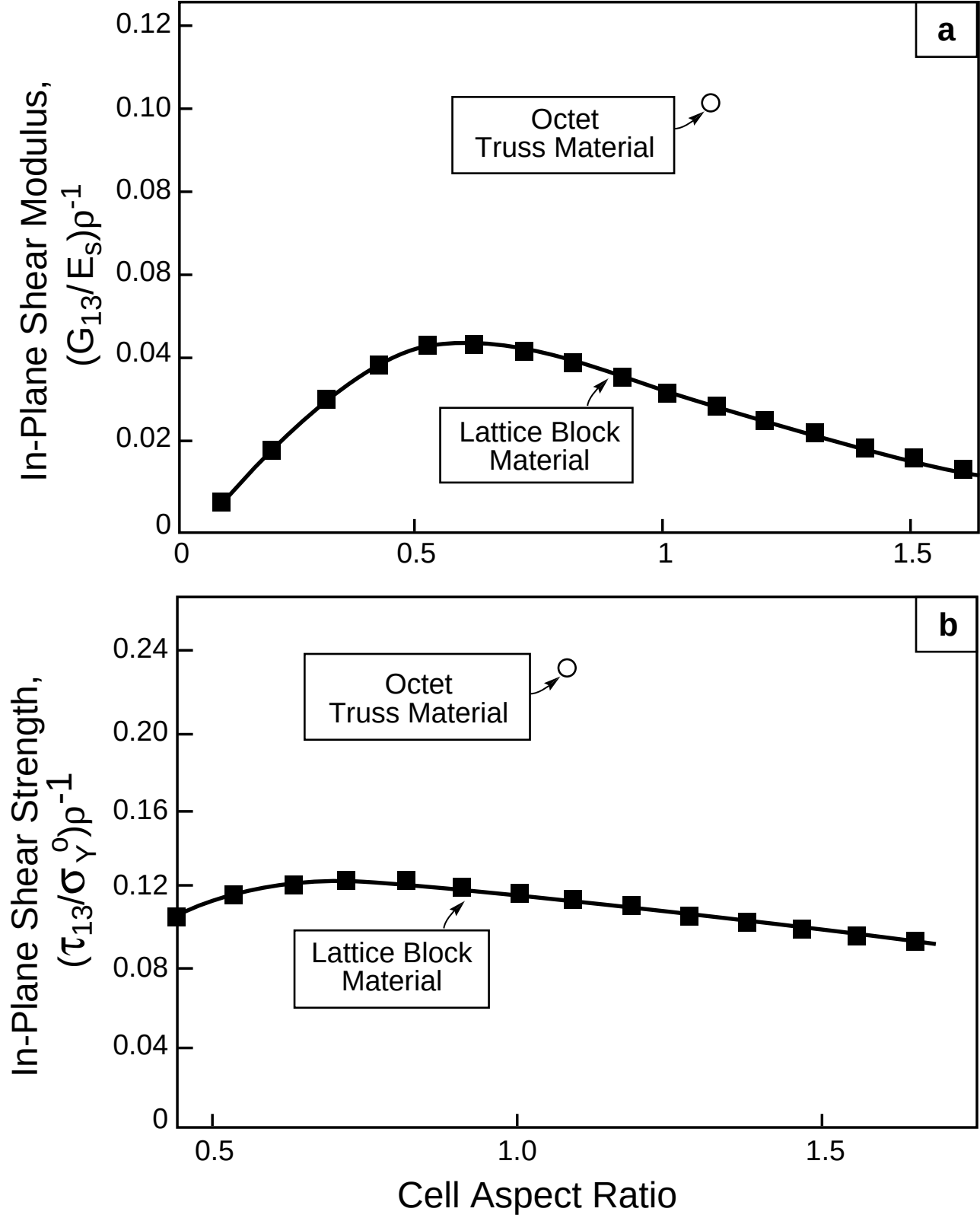


Figure 11

Benchmarks.Fig.#11a

# LINEAR MATERIALS

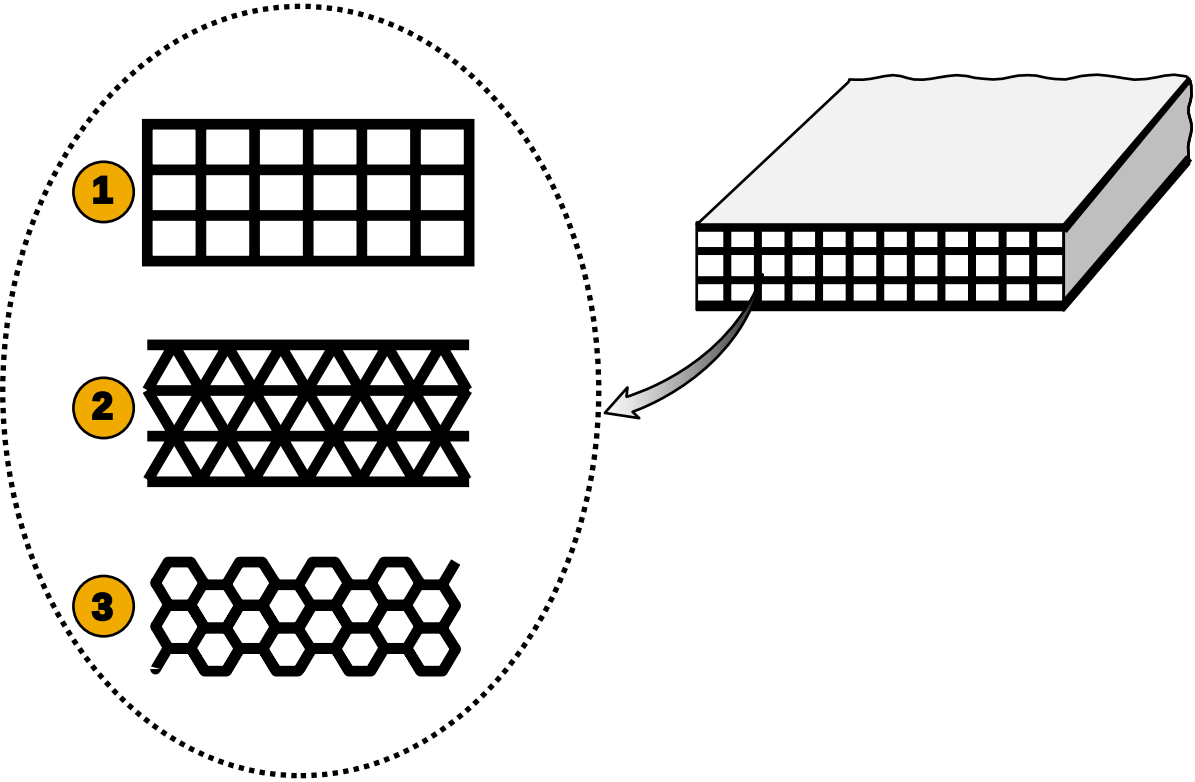


**Core Configuations**

Figure 12

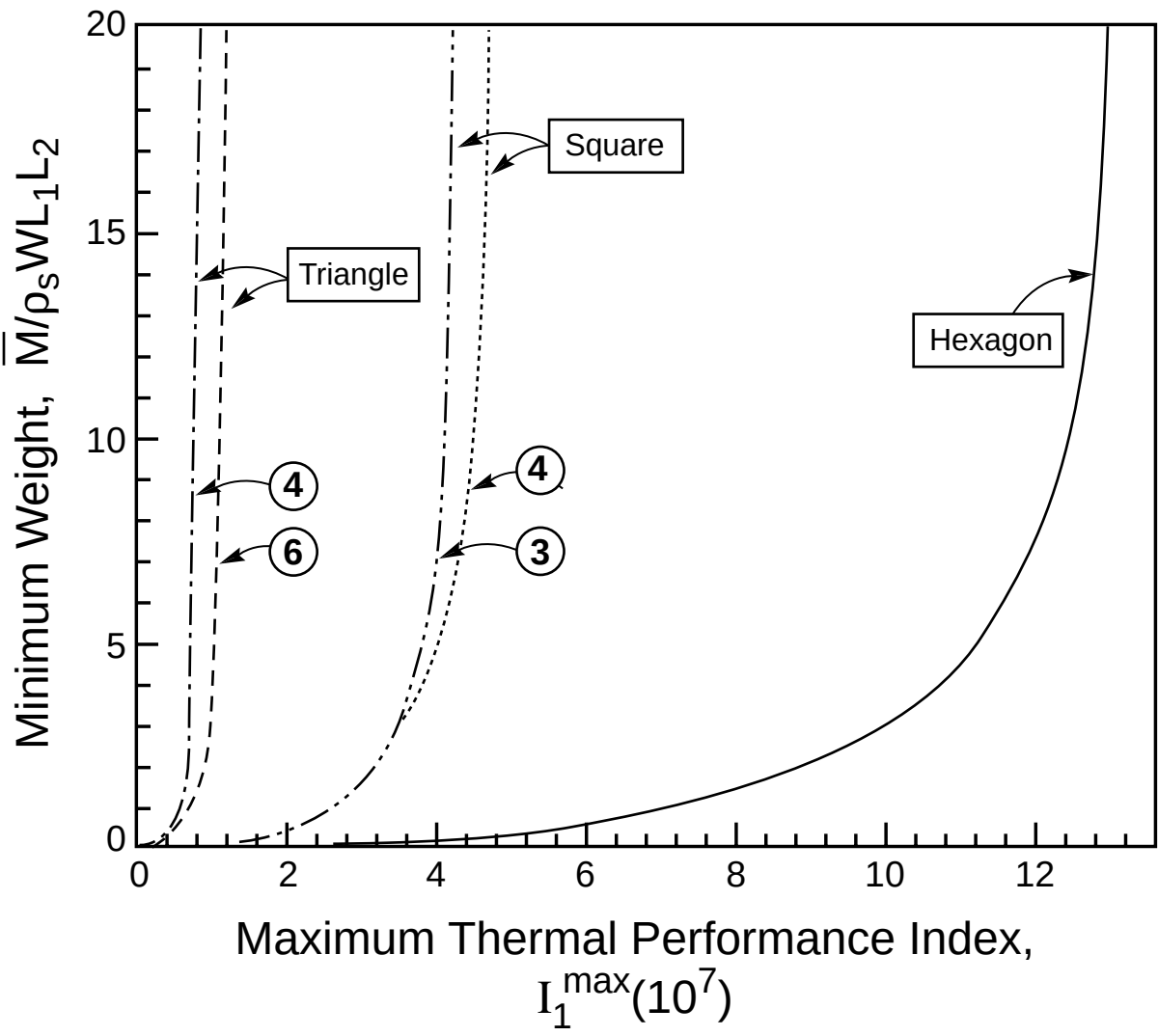
20
15
10
5
0
0
2
4
6
8
10
12
Minimum Weight, $\overline{M}/\rho_S W L_1 L_2$
Maximum Thermal Performance Index, $I_1^{max}(10^7)$
Square
Triangle
Hexagon
4
6
4
3

Figure 13

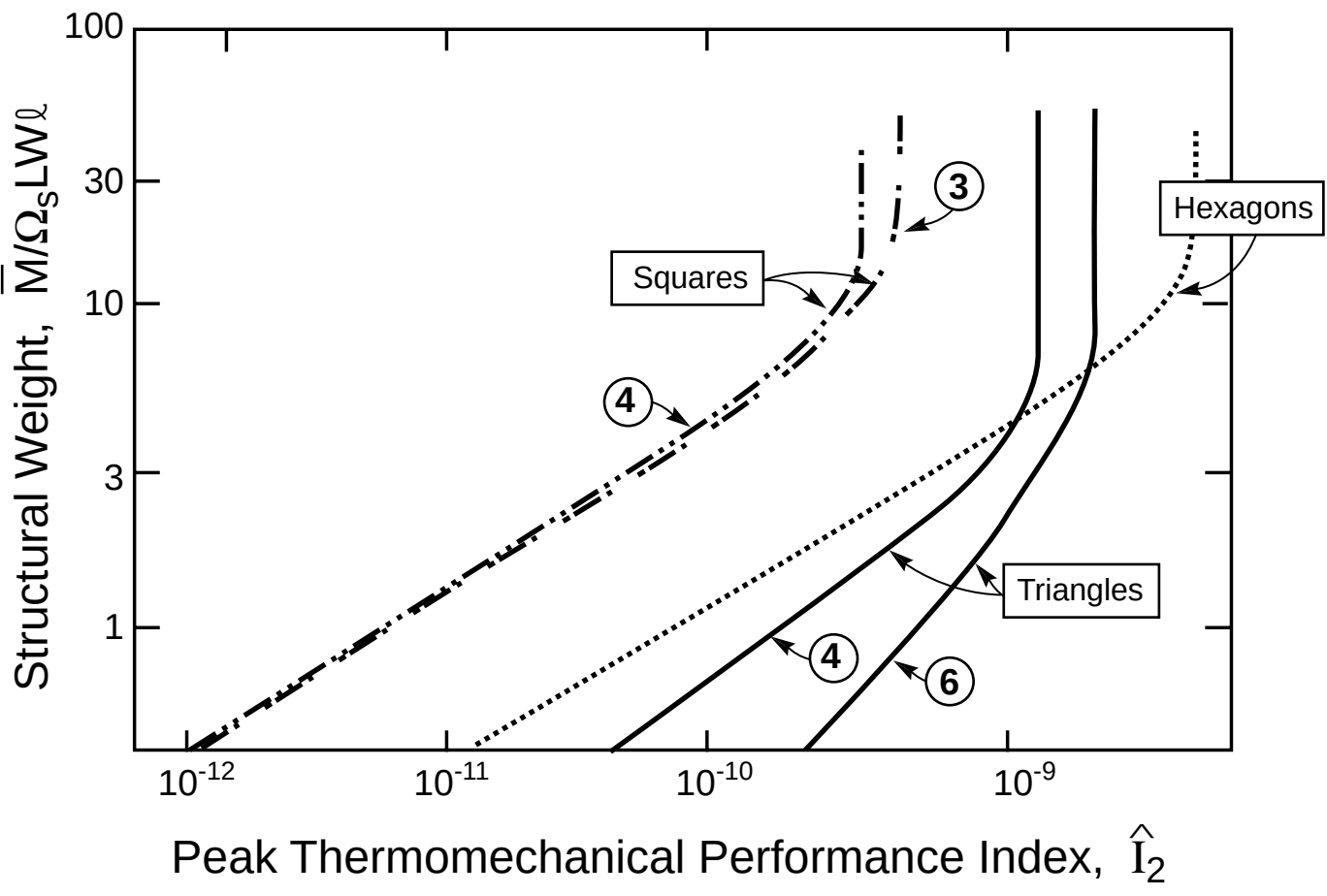
100
30
10
3
1
Structural Weight, $\bar{M}/\Omega_s LW\ell$
Squares
Hexagons
Triangles
3
4
4
6
$10^{-12}$
$10^{-11}$
$10^{-10}$
$10^{-9}$
Peak Thermomechanical Performance Index, $\hat{I}_2$

Figure 14

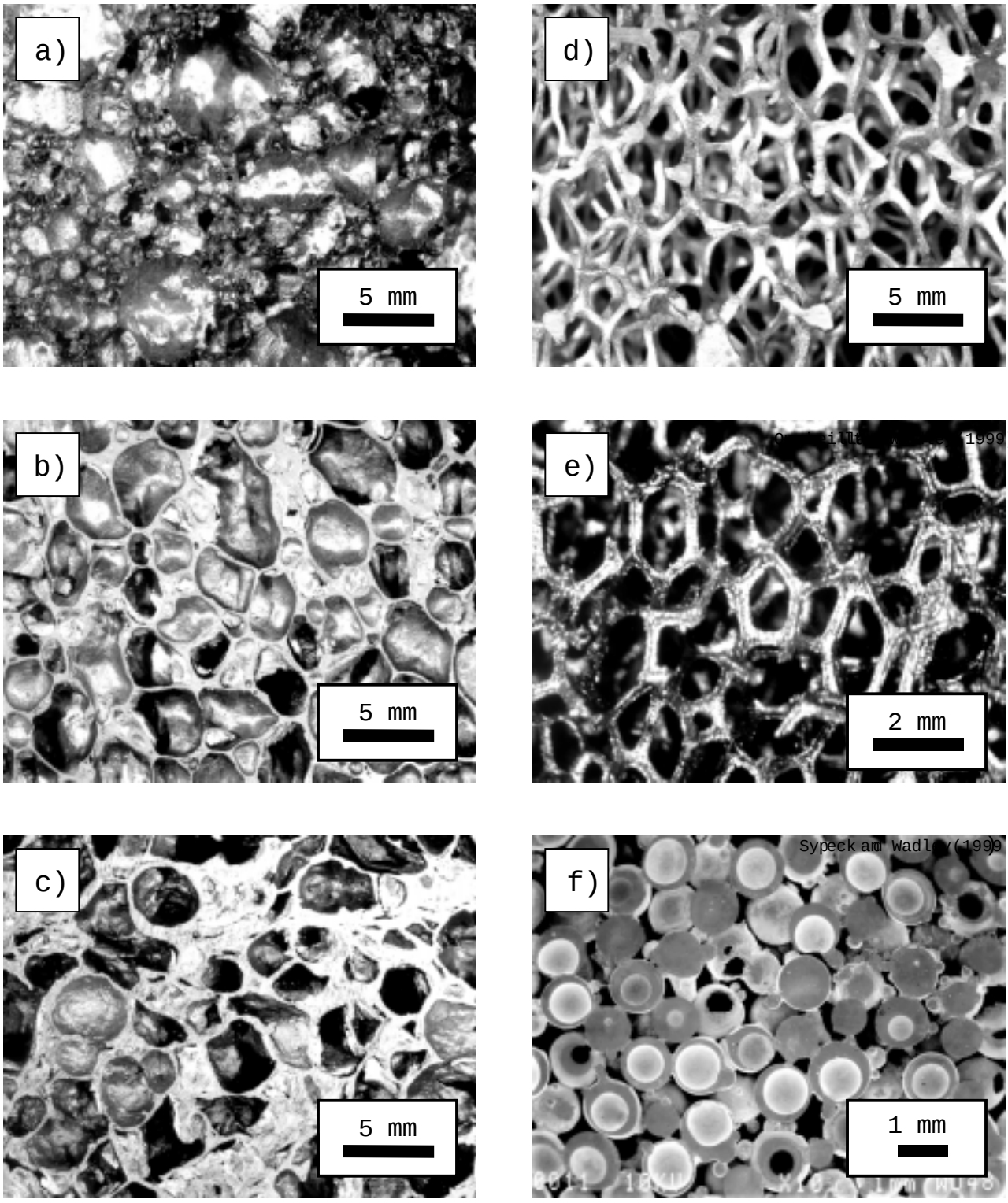


Fig 15

# MELT GAS INJECTION

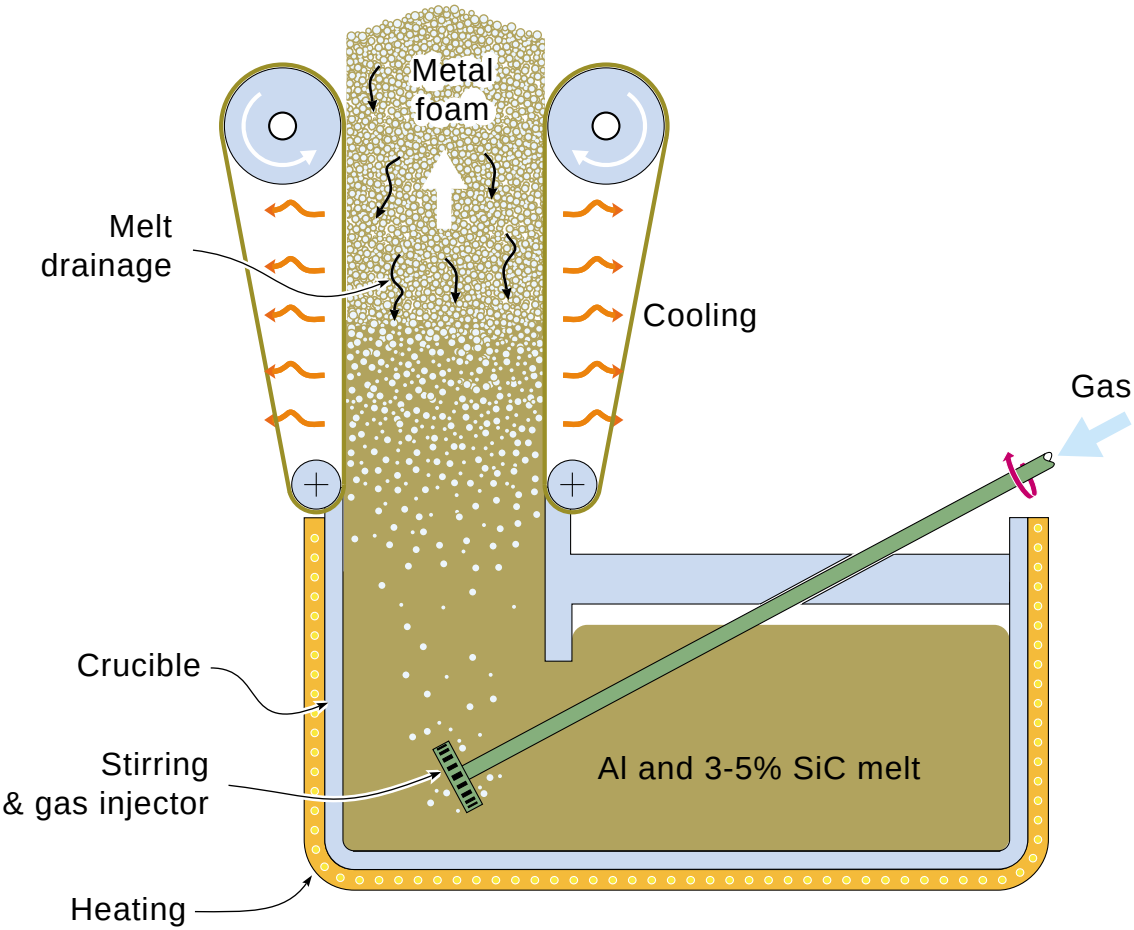


**Fig. 16a**

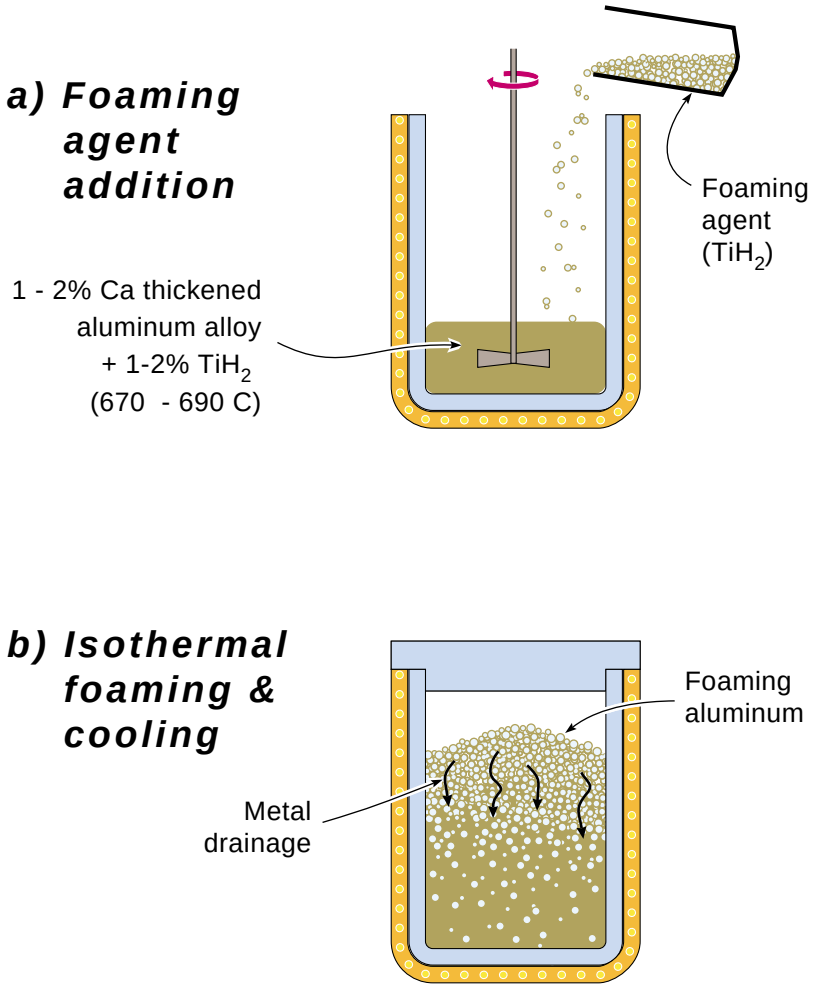
a) Foaming agent addition
1 - 2% Ca thickened aluminum alloy + 1-2% $TiH_2$ (670 - 690 C)
Foaming agent ($TiH_2$)
b) Isothermal foaming & cooling
Foaming aluminum
Metal drainage

**Fig 16b**

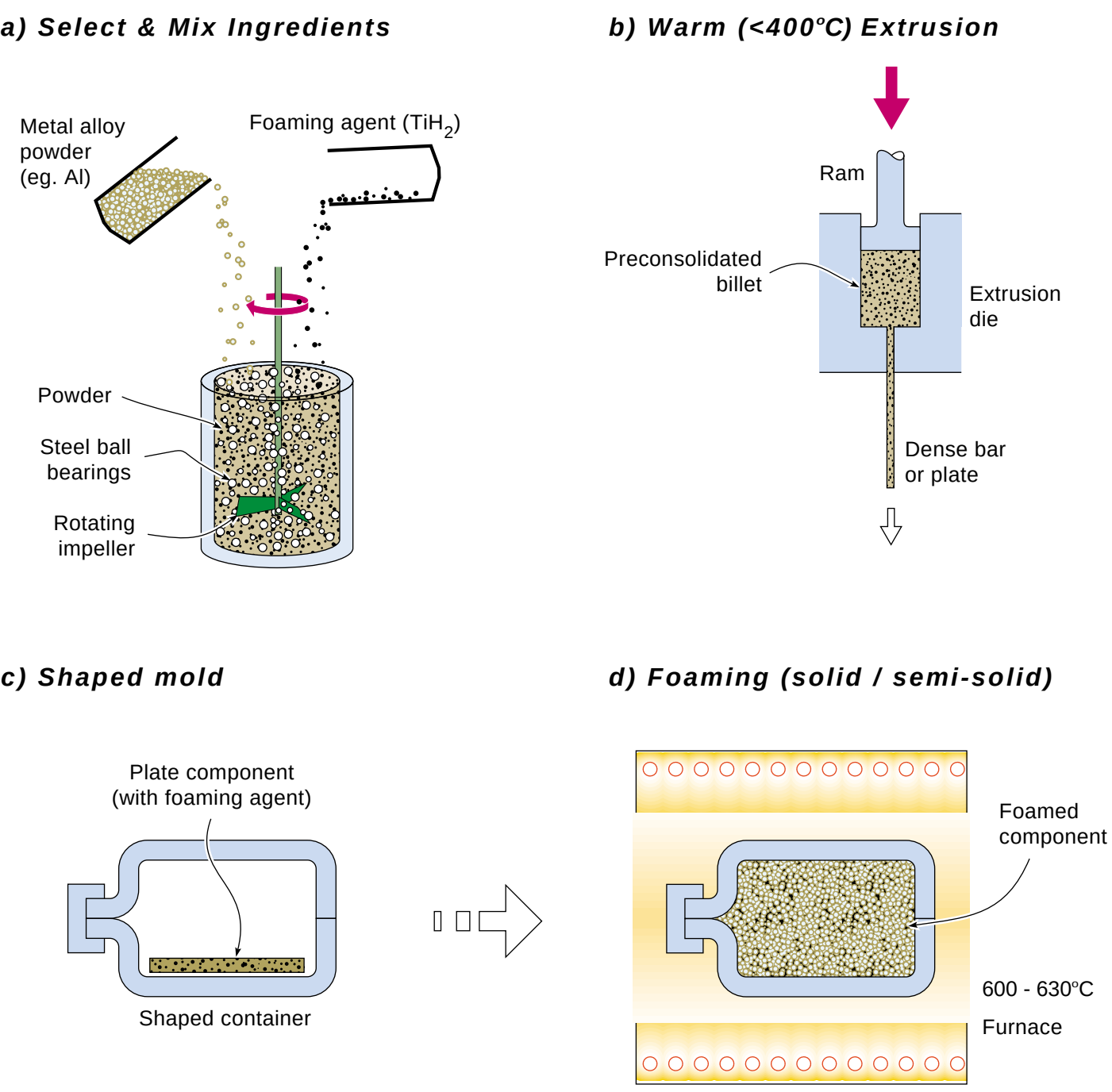
a) Select & Mix Ingredients
Metal alloy powder (eg. Al)
Foaming agent ($TiH_2$)
Powder
Steel ball bearings
Rotating impeller
b) Warm (<400°C) Extrusion
Ram
Preconsolidated billet
Extrusion die
Dense bar or plate
c) Shaped mold
Plate component (with foaming agent)
Shaped container
d) Foaming (solid / semi-solid)
Foamed component
600 - 630°C
Furnace

**Fig 16c**

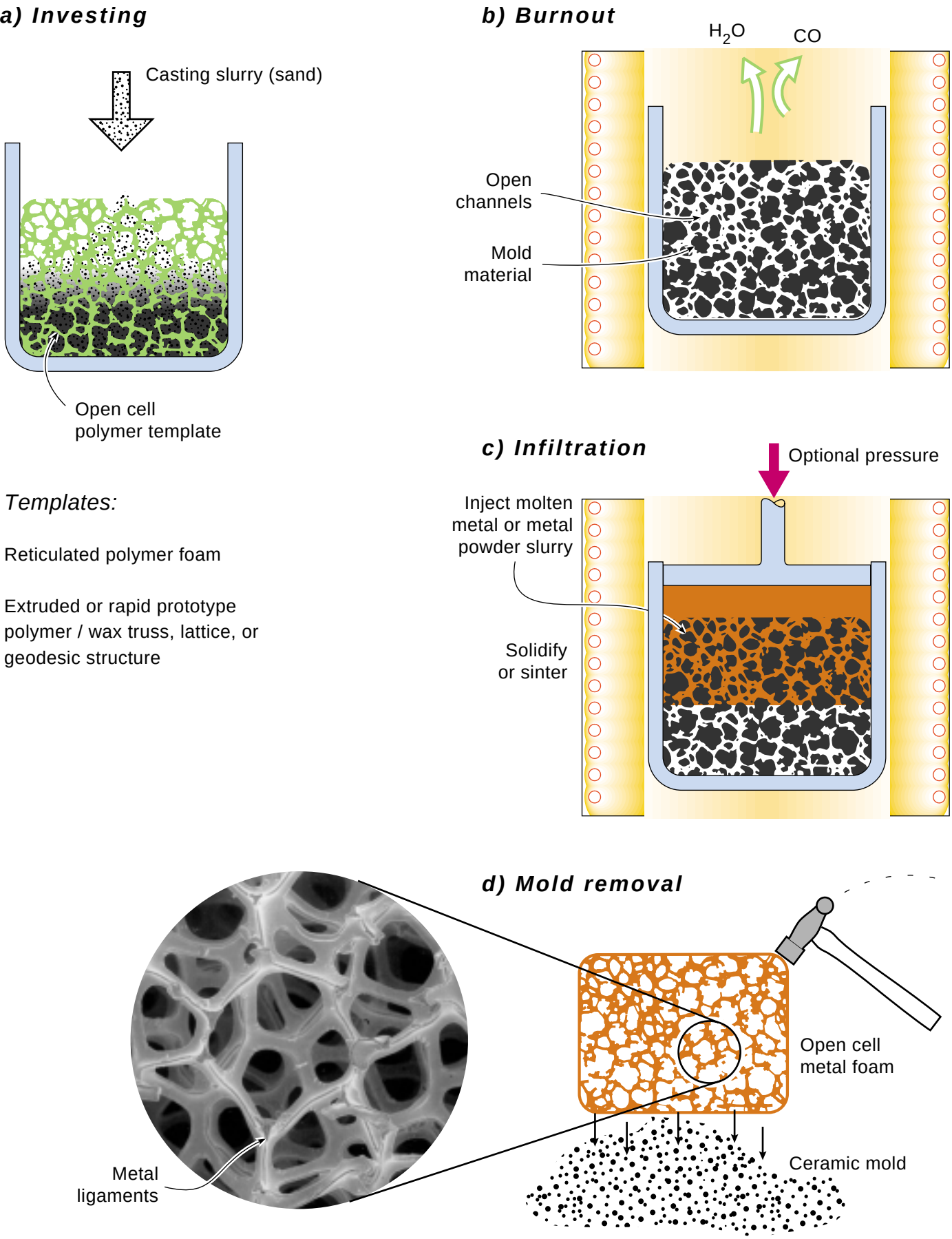


*Templates:*

Reticulated polymer foam

Extruded or rapid prototype polymer / wax truss, lattice, or geodesic structure

Fig 17

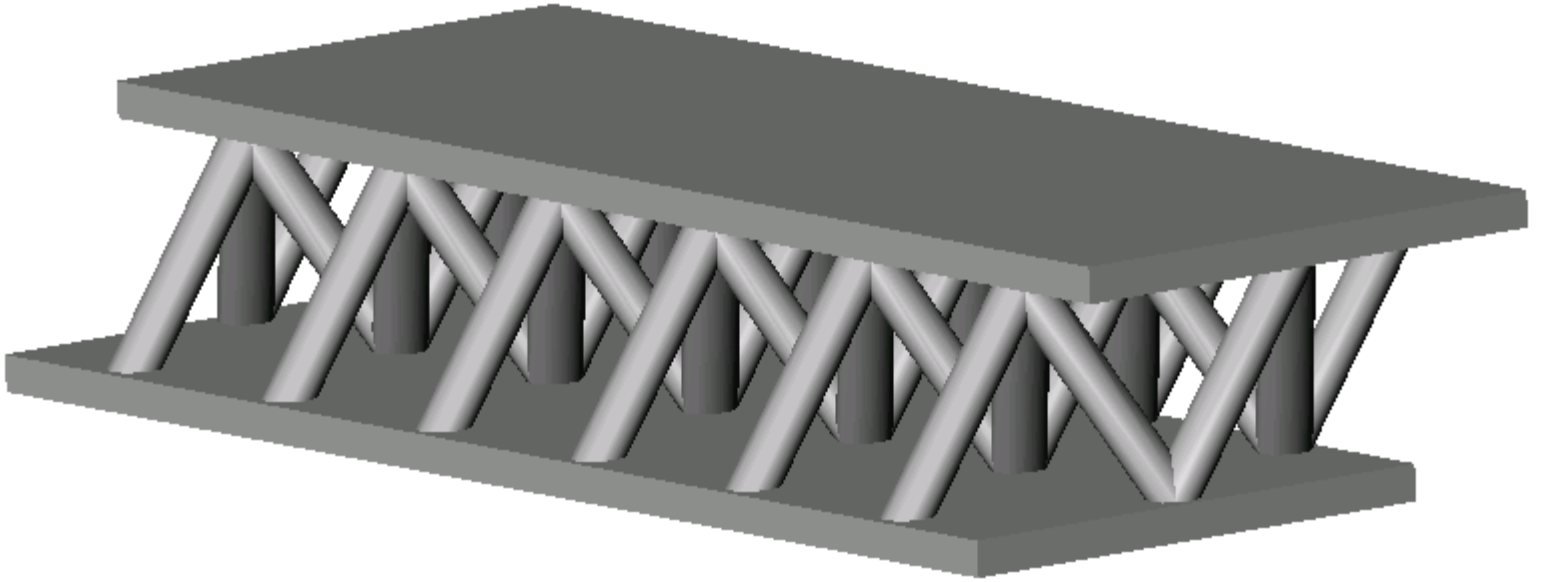

**Fig. 18**

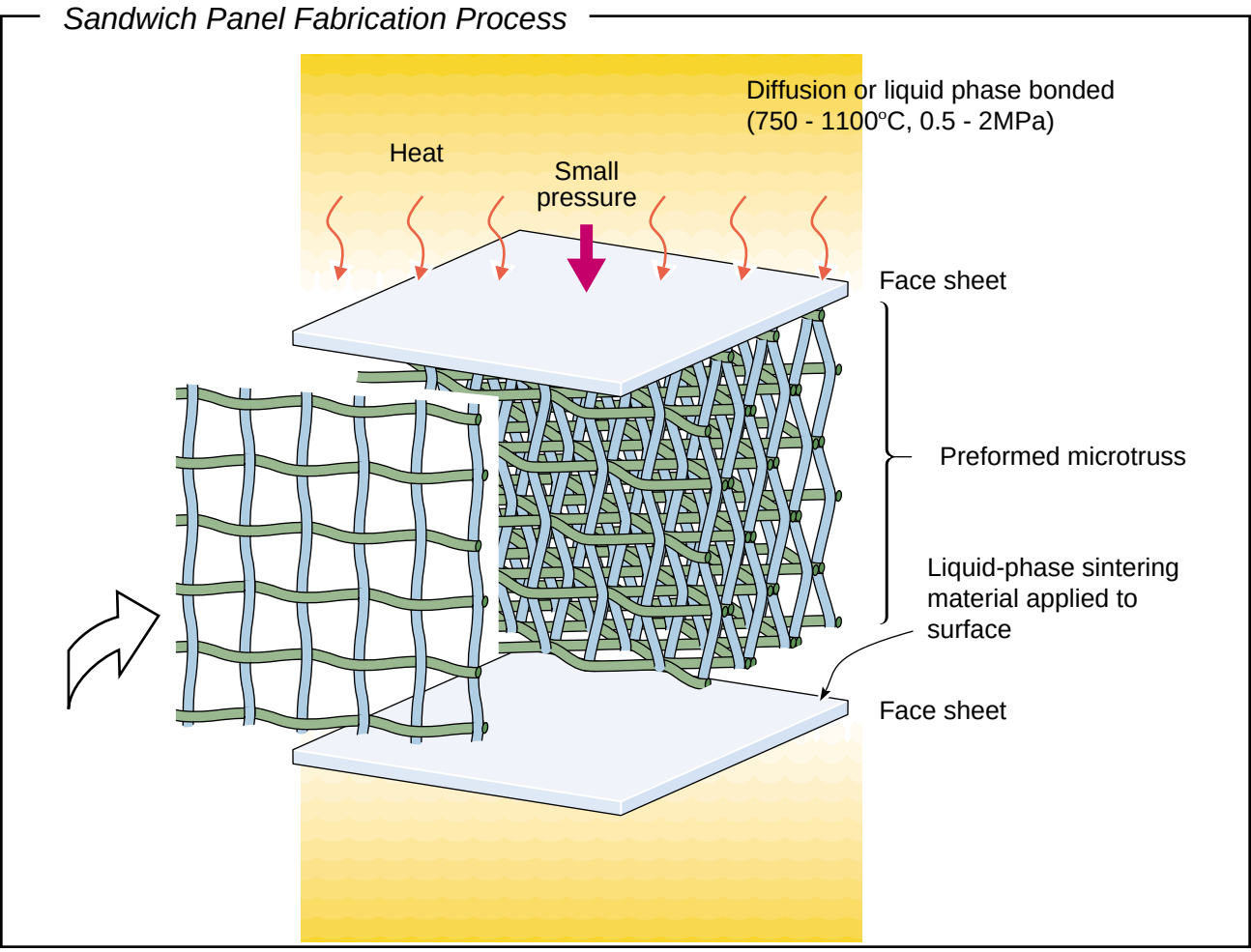
Sandwich Panel Fabrication Process
Diffusion or liquid phase bonded
(750 - 1100°C, 0.5 - 2MPa)
Heat
Small
pressure
Face sheet
Preformed microtruss
Liquid-phase sintering
material applied to
surface
Face sheet

**Fig 19a**

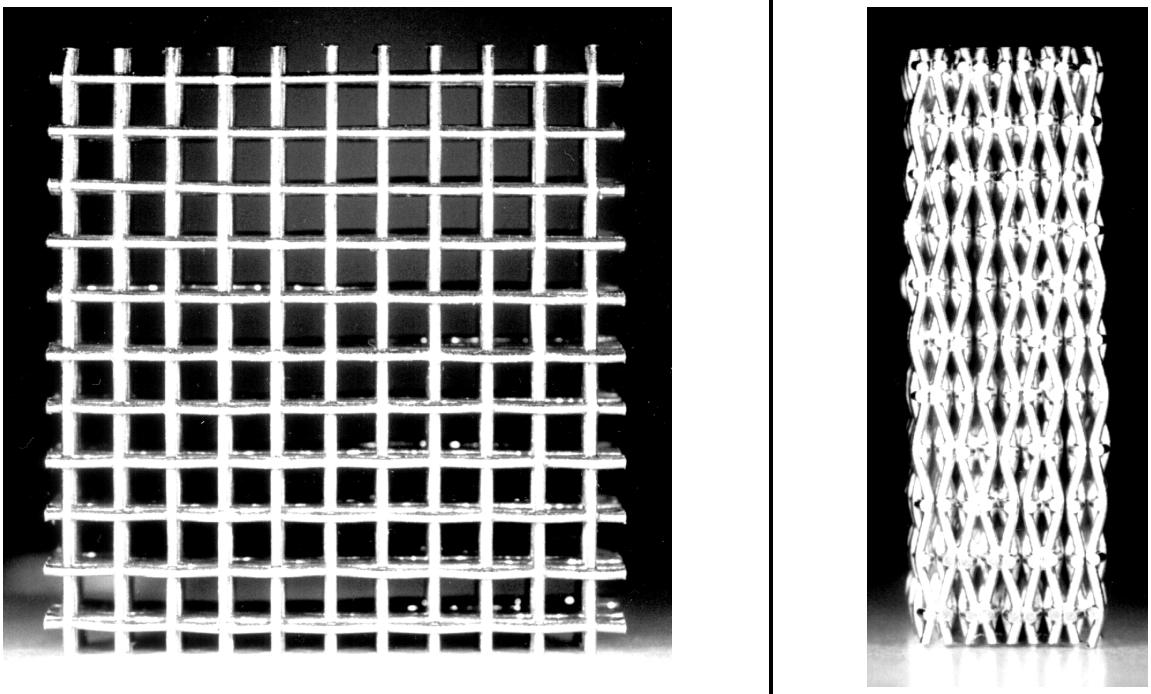

**Front** **Side**

**Sypeck and Wadley (2000)**

12.7 mm

Fig 19b